ISSN Application No. 21823

An EP Journal on Architectural Education

Volume No. 11

Issue No. 3

September - December 2023

ENRICHED PUBLICATIONS PVT. LTD

S-9, IInd FLOOR, MLU POCKET,
MANISH ABHINAV PLAZA-II, ABOVE FEDERAL BANK,
PLOT NO-5, SECTOR-5, DWARKA, NEW DELHI, INDIA-110075,
PHONE: - + (91)-(11)-47026006

ISSN Application No. 21823

An EP Journal on Architectural Education

Aims and Scope

An EP Journal on Architectural Education is a National Journal. It Publishes Original Research Papers in Different Areas of Architecture Education. It Publishes 3 Issues in a Year from 2018 in purpose of enhancing architectural scholarship in design, history, urbanism, cultural studies, technology, theory, and practice.

ISSN Application No. 21823

An EP Journal on Architectural Education

Managing Editor
Mr. Amit Prasad

Editorial Board Member

Dr. Prabhjot Kaur
GZS College of Engineering &
Technology Bathinda
pkaurdap@gmail.com

ISSN Application No. 21823

An EP Journal on Architectural Education

(Volume No. 11, Issue No. 3, September - December 2023)

Contents

A mixture of Ethanolic Solution of Magnetic Studies of Some Transition Metal Complexes

Dr. Radhika Raman Singh
Department of Chemistry, D. S. S. V. College,
Simri, Buxar

ABSTRACT

A number of new mixed ligand complexes of Co(II), Ni(II), Cu(II) and Zn(II) containing diphenylamine- 2-carboxylic acid (DPHC) and furfural dine-2- amino thiazole (FAT) have been synthesized and characterized by elemental analysis, TLC, conductivity measurements and IR spectral data.

Key Words: Synthesis, Transition metal, Complexes, Diphenylamine, Schiff base.

Complexes besides being academically important[1] have assumed analytical[2], industrial[3], pharmaceutical, medical, toxicological[4] and biochemical importance[5]. The metal complexes of nitrogen containing ligands have been found more biologically active[6] in comparisons to the ligand having other donor sites.

The present paper describes the mixed – ligand complexes[7] of M^{2+} ions (M=Co(II), Ni(II), Cu(II), Zn(II) with diphenylamine-2-hydroxy-2-carboxylic acid as primary ligand and furfural dine-2-aminothiazole as secondary ligand.

(a) Synthesis of diphenylamine-2-hydroxyle-2-carboxylic acid (DPHC): Both o- chlorobenzoic acid (0.003M) and o-aminophenol (0.003M) were taken in 1:1 molar ratio in 100ml distilled water in flask fitted with a water condenser. The mixture was slightly alkaline with K2CO3 solution and a little copper oxide was added to it. The contents were refluxed on water – both for about 5 h . After decolorizing with charcoal, the contents were filtered, concentrated and cooled. The obtained solution was acidified with dilute HCL in excess till the precipitation of the resultant product was complete. It was filtered in cold, dried and re- crystallized from alcohol to obtain a brown powder.

(b) Synthesis of furfural dine- 2-aminothiazole (FAT): A mixture of furan – 2 – aldehyde 1.70ml (2 x 10^{-2} mole) and 2- aminothiazole 2.0g (2 x 10^{-2}mole) in 50 ml dry ethanol was dissolved and refluxed for 12h over a water- bath. The solution thus obtained was cooled at room temperature and the excess of ethanol was almost distilled off under pressure. On keeping the obtained viscous solution at room temperature for one week a solid product was obtained. It was washed with acetone followed by ether and finally re- crystallized from methanol and dried.

SYNTHESIS OF METAL COMPLEXES

A mixture of ethanolic solution of metal acetates [0.10g $(AcO)_2$ Cu H2O) 0.12g $(AcO)_2$ Ni 4H2O, 0.13g $(AcO)_2$ Co.H_2O, 0.11g $(AcO)_2$ Zn. 2H_2O] DPHC (0.13g X 10^{-4} mole) and FAT (0.98g, 5 x 10^{-4}mole) was refluxed for 3h after maintaining PH ca,6. On cooling, the complex precipitated out, which was filtered, wased with ethanol and dried in a vacuum desiccators over anhydrous $CaCl_2$.N, S and metal in complexes were determined by the standard method[9] C and H analyses were performed (table-1).Molar conductance was measured in 10- M3 dry DMF solution using Toshniwal Conductivity bridge; IR spectra were recorded on Perkin- Elmer Model 577 (Table- 2). Antimicrobial data was shown in table- 3

RESULT AND DISCUSSION

Analytical data of complexes suggest their 1: 1: 1(MLL) stoichiometry and the conductivity measure ment reveal their non- electrolytical nature.

The ligand DPHC revealed characteristic IR band one at 3010cm^{-1} and 1750cm^{-1} (>OH and >C=O carboxylic stretching vibration). In the IR spectra of metal complexes, the band due to (- NH) is shifted to negative side by 30- 40 cm^{-1} which indicates the involvement of this ligand in bonding with metal ions through nitrogen atom. The OH band of carboxylic group disappeared on complexation with metal ions due to the deprotonation from (M_ OOC) bond. Another ligand FAT exhibits IR bands at 1650 cm^{-1} (>C = N azometine stretching), 1485 cm^{-1} and 1525 cm^{-1} (breathing vibration of thiophene and furan ring) in the lower frequency region showing the coordination of metal with ligand. Some new band corresponding to (M-O), (M- N), (M-S) also present in the IR spectra of the complexes respectively at 550, 445 and 335 cm-1 which further support the chelation the two ligands with metal ions through the coordination site. The ligands and there metal complexes were screened for antibacterial and antifungal activities against two bacterial, staphylococcus aureus and Escherichia coli and two common fungi. Aspergillus and Candida albicans, by serial dilution method.

TABLE – 1 PHYSICAL AND ANALYTICAL DATA OF SYNTHESIZED COMPOUND

Compound (m. f)	Colour	Mw Found (Calcd.)	m.p/d.p. (^{o}C)	% Analysis Found (Calcd.)				
				C	H	N	S	M
DPHC ($C_2H_{11}NO_3$)	Brown	245 (229)	144	69.20 (68.11)	4.93 (4.80)	5.91 (6.12)	-	-
FAT ($C_8H_6N_2O_s$)	Brown	196 (178)	126	54.52 (53.93)	3.86 (3.37)	15.26 (15.73)	17.72 (17.91)	-
CO(II)-DPHC- FAT ($C_{21}H_{16}O_4N_3SNi$)	Blackish Brown	396 (376)	270	38.60 (38.32)	5.55 (5.05)	10.57 (11.17)	8.11 (8.51)	0.644 (0.156)
Ni(II)-DPHC- FAT ($C_{21}H_{16}N_3O_4SNi$)	Brown	400 (376)	250	38.64 (37.32)	5.58 (5.07)	10.67 (11.17)	8.08 (8.51)	0.648 (0.156)
Cu(II)-DPHC- FAT ($C_{21}H_{16}N_3O_4SCu$)	Brownish Black	410 (381)	260	38.09 (37.79)	5.40 (4.98)	10.52 (11.02)	7.89 (8.39)	15.99 (16.79)
Zn(II)- DPHC- FAT ($C_{21}H_{16}N_3O_4SZn$)	Brown	405 (381)	230	38.15 (37.89)	5.37 (5.00)	11.73 (11.03)	7.92 (8.42)	15.67 (16.57)

TABLE -2 KEY INFRARED SPECTRAL BANDS (Cm^{-1}) OF METAL COORDINATION COMPOUNDS

DPHC	FAT	CO(II) DPHC- FAT	Ni(II) DPHC- FAT	Cu(II) DPHC- FAT	Zn(II) DPHC- FAT	Probable assignments
3350	-	-	-	-	-	V(OH)(phnolic)
3300	-	-	-	-	-	V(OH)(carboxylic)
3010	-	2990	2995	2990	2995	V(NH)
1750	-	1720	1725	1725	1730	>C=O(Carboxylic)
-	1625	1615	1610	1615	1610	>C=N(azomethine stretching)
-	1525	1510	1510	1515	1505	Breathing vibration of furan ring
-	1485	1475	1470	1465	1460	Breathing vibration of thiophene ring
-	-	545	540	540	535	v(M- o)
-	-	440	445	435	440	v(M-N)
-	-	335	340	335	340	v(M- S)

TABLE -3 ANTIMICROBIAL ACTIVITY DATA (MIC VALUES) IN MOLAR CONCENTRATION (X 10^{-5}) OF SYNTHESIZED COMPOUNDS

S. No	Compund	Bacterial		Fungi	
		S. aureus	E.coli	A. nidulans	C. albicans
1	DPHC	20.80	20.80	41.60	41.60
2	FAT	7.20	7.20	14.40	14.40
3	Co(II)-DPHC-	4.82	4.82	9.64	9.64
4	Ni(II)- DPHC-FAT	4.80	4.80	9.60	9.60
5	Cu(II)- DPHC-FAT	4.70	4.70	9.40	9.40
6	Zn(II)- DPHC - FAT	4.81	4.81	9.62	9.62
7	Standard	4.36	4.36	8.30	8.30

Abbreviation: S. aureus - Staphylococcus aureus, E. coli - Escherichia coli A. Nidulans - Aspergillus nidulans, C. albicans- Candida albicans.

REFERENCES

1.B.E.Fisher and H. Siegal, J.Am. Chem. Soc.102, 2998(1980)

2. F.A.Cotton and G.wilkinson, Advanced Inorganic Chemistry: A Comprehensives text,4th Edn. John Wiley & sons, New York (1980)

3. G.R Choppin, Eur. J. Solid State Inorg. Chem, 28,319 (1991)

4. T.V.R.K.Rao and B.N.Das, J.Inst. Chemists, 70,5 (1998)

5. Firoz Khan and Farid Khan, J.Indian Chem.Soc, 74,171 (1997)

6. S.S.Massud and H. Siegal, Inorg. Chem, 110,6857 (1998)

7. Maria Pleniceanu, Loan Burnea, Maria Isvoranu, Cezar Spinu and Elena Glodeanu.J.Indian Chem. Soc; 76, 308(1999)

8. B. Singh and H. Mishra J. Indian Chem. Soc,63, 1069 (1986)

A New Characterization of Semi Open Set in Topological Space

Reema Bahan*, Dr. Ravindra Nath Pandey**
Department of Mathematics
*Department of Mathematics Patna University, Patna – 800005, Bihar, India.
**Ex prof. &H.O.D Department of Mathematics ,Patna University

A B S T R A C T

This paper presents the study of some new results on properties of open set in Topological space. Here, we consider usual Topology R which is neither open nor closed in R and here, it is proved that the set is semi open but not open, closed, pre- open or pre-closed.

KEYWORDS : Discrete Space , Open Set, Semi – open set, Union set. Interior, Closure, Complement, Topological space

INTRODUCTION :

Bahan, R (1) and Prasad, D (6) are the pioneer workers of the present area. In fact, the present work is the extension of work done by Ferrer, J(2), Jha M.N. et al (3), Kelly et al (4), Levine. N(5) and Santi Leela et al (7). In this paper, we have studied a new characterization of semi open set in Topological space.

Here, we use the following Notations, definitions and Fundamental Ideas.

Notations

$\text{Int.(cl(A))} \equiv$ The Interior of the closure of the set

$\overset{0}{\underset{}{A}} \equiv$ The Interior of the closure of the set A.

$\text{Cl(Int.(A))} \equiv$ The closure of the interior of A.

$A^c \equiv$ Complement of the set A.

DEFINITION

1. SEMI-OPEN SET :

Let $A \subseteq X$, a topological space. The A is a semi-open set if $A \subseteq Cl(Int.(A))$.

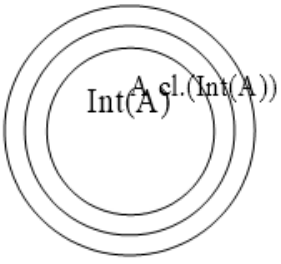

Example (1.1) :

Let A= (a ,b) in R with usual topology, which is neither open nor closed in R.

Proof:

Since Int (A) = (a, b)

$\Rightarrow$ Cl(Int.(A)) = Cl((a, b)) = [a, b] $\supseteq$ A

$\Rightarrow$ A $\subseteq$ Cl(Int.(A))

Therefore A is semi-open.

So a semi-open set may not be open or closed.

Further

Since Cl(Int(A)) $\not\subseteq$ A

Therefore A is not pre-closed.

Also Cl(A) = [a, b]

$\Rightarrow$ Int(cl(A)) = (a, b) $\not\supseteq$ A

$\Rightarrow$ A $\not\subseteq$ Int(cl(A))

Therefore A is not pre-open.

Thus a set may be semi open but not open, closed, pre-open or pre-closed.

Example (1.2) :
Let A = (a, b] be in R with usual topology then A is semi-open.

Proof:

Since Int(A) = (a, b)

$\Rightarrow$ Cl(Int(A)) = [a, b] $\supseteq$ A

$\Rightarrow$ A $\subseteq$Cl(Int(A))

Therefore A is semi-open

Example (1.3) :
Consider discrete space X. Since every subset is open, it is semi-open.

Example (1.4) :

Let X = {1, 2, 3}

T = {ϕ, X, {1}, {2}}

Let A = {1, 3}

Then Int(A) = {1}

$\Rightarrow$ Cl(Int(A)) = {1, 2, 3} = X $\supseteq$ A

$\Rightarrow$ A $\subseteq$Cl(Int(A))

Therefore A is semi-open.

It is also a pre-open set.

Example (1.5) :

Consider indiscrete space X and $\phi \subset A \subset X$.

Since Int(A) = ϕ

$\Rightarrow Cl(Int(A)) = \phi \not\supseteq A$

$\Rightarrow A \not\subseteq Cl(Int(A))$

Therefore A is not semi-open.

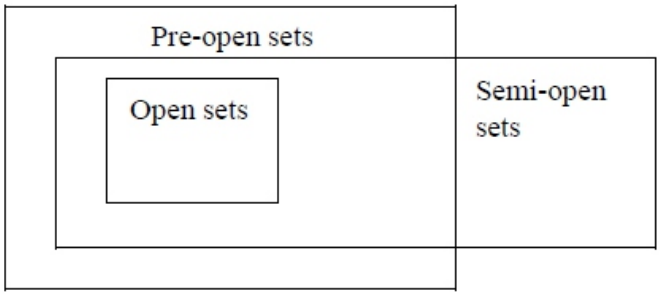

2. MATHEMATICAL TREATMENT OF THE PROBLEM:-

2.1 Let A be semi-open. Then there exists an open set G such that

$G \subseteq A \subseteq \overline{G}$

Proof:

Let A be semi-open, then $A \subseteq \overline{IntA}$

Therefore $IntA \subseteq A \subseteq \overline{IntA}$

Let G = IntA, then G is open.

Also $G \subseteq A \subseteq \overline{G}$ (By Using Property)

2.2 An open set is semi-open.

Proof:

Let A be open.

Then A = Int(A)

$\Rightarrow A \subseteq cl(Int(A))$

Therefore A is semi-open

2.3 A' is a semi open set $\Leftrightarrow$A is semi-closed set.

Proof:

Let A' be a semi-open set, then

$A' \subseteq \overline{IntA'}$

But $\overline{A} = (IntA')'$

$$\text{Hence } \overline{\text{Int}A'} = \left(\text{Int}\left(\text{Int}A'\right)'\right)'$$

$$\text{Therefore } A' \subseteq \left(\text{Int}\left(\text{Int}A'\right)'\right)'$$

Therefore A is semi-open.

It is also a pre-open set.

Example (1.5) :

$$\Rightarrow A \supseteq \text{Int}\left(\text{Int}A'\right)' = \text{Int}\bar{A}$$

Therefore A is a semi-closed set.

Since all steps can be reversed.

So A is semi-closed $\Rightarrow A'$ is semi-open.

Corollary (2.1)

A is semi-open set $\Leftrightarrow A'$ is a semi-closed set.

2.4 Union of an arbitrary family of semi-open sets is semi-open.

Proof:

Let $\{A_i\}$, $i \in I$ be a family of semi-open sets.

Then $A_i \subseteq \overline{\text{Int}A_i}, \forall i$

Now $A_i \subseteq \cup_i A_i$

$$\Rightarrow \text{Int}\left(A_i\right) \subseteq \text{Int}\left(\cup A_i\right)$$

$$\Rightarrow \overline{\text{Int}A_i} \subseteq \overline{\text{Int}\left(\cup A_i\right)}$$

Therefore $A_i \subseteq \overline{\text{Int}\left(\cup A_i\right)}, \forall i$

$$\Rightarrow \cup A_i \subseteq \overline{\text{Int}\left(\cup A_i\right)}$$

Therefore $\cup A_i$ is semi-open.

Main Result

Let A be semi-open in the topological space X and suppose $A \subseteq B \subseteq \text{cl}(A)$ *. Then B is semi-open.*

Proof :

There exists an open set G such that $G \subseteq A \subseteq \text{cl}(G)$.

Now $A \subseteq B$

Therefore $G \subseteq A \subseteq B$

$\Rightarrow G \subseteq B$

But $A \subseteq cl(G)$

$\Rightarrow cl(A) \subseteq cl(G)$

and thus $B \subseteq cl(A) \subseteq cl(G)$

Therefore $G \subseteq B \subseteq cl(G)$

Hence B is semi-open.

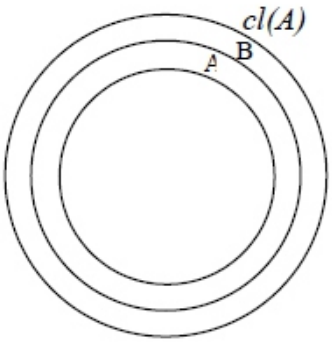

Hence the Result.

ACKNOWLEDGMENT :

The authors are thankful to Prof.(Dr.) S.N.Jha, Ex. Head, Prof. (Dr.) P.K. Sharan, Ex. Head and Prof. (Dr.) B.P. Singh Present Head of the University Deptt. of Mathematics, B.R.A.B.U. Muzaffarpur, Bihar, India and Prof. (Dr.) T.N. Singh, Ex. Head, Ex. Dean (Science) and Ex. Chairman, Research Development Council, B.R.A.B.U. Muzaffarpur, Bihar, India for extending all facilities in the completion of the present research work.

REFERENCES

1. *Bahan, R., Pandey, R.N. and Chadra, P. : Pre-continuous mapping, Jour. PAS. . Ferrer, J., Gregory, V. and Alegre, C. : Extensions of Semi-continuous functions, Indian J. Pure appl. Math. 26(2), 103-112, February, 1995.*
3. *Jha, M.N. and Shukla, R. : On some topological spaces, Ph.D. Thesis, Patna University, August (1967).*
4. *Kelley, J.L. : General Topology, Van Nostrand Pinceton, N.J. (1955).*
5. *Levine, N. : Semi-open sets and semi-continuity in Topological spaces, Amc. Math. Monthly, Vol. 70, p. 36-41, (1963).*
6. *Prasad, D. and Bahan, R. : Some properties of pre-open and pre-closed set, Jour. BMS, Vol. 24, p. 67-72 (2004).*
7. *Santi Leela, D. and Balasubramanian, G. : Some what semi-continuous and some what semi- open functions Bull. Cal. Math. Soc., 94(1), 41-48 (2002)*

A Kinetic Study of Dielectric Effect of Water Ethanol Reaction Media on the Biochemical Potential of Solvolytic Products of Higher Propionate

Rajiv Kumar[1], R. T. Singh[2]

[1]Research Scholar, Dept of Chemistry, V.K.S. University, Ara

[2]Professor & HOD Chemistry and The Dean of the Faculty of Science, V. K. S. University, Ara

ABSTRACT

The dielctric effect of aquo-ethanol reaction media on the Biochemical potential of propionate ester was highlighted by studying the kinetics of alkali catalysed hydrolysis of butyl propionate in it(reaction media). From simultaneous increase in all the three thermodynamic parameters i.e. ΔH^*, ΔS^* and ΔG^*, it may be inferred that the solvent ethanol acts as enthalpy stimulator and entropy controller. From evaluated numerical value of Iso- kinetic temperature of the reaction i.e. 309.0, it is concluded that aquo-ethanol media may be used for manufacturing powerful ointment for removing skin diseases from the hydrolytic product of propionate ester.

KeyWords- Biochemical, Potential Solvolytic Products Higher Propionates, Dielectric Effect, Iso-composition, Iso-Dielectric, Iso-kinetic, Barclay-Butler Rule, Strong Interaction

INTRODUCTION :

The studies in the kinetics of alkali catalysed hydrolysis of butyl propionate in aquo-ethanol media were proposed as the solvent effect of dipolar-Protic solvent ethanol on the biochemical potential propionate esterhas not been paid even primary attention by the kineticists so far. It has been planned to study the kinetics of the solvolysis of butyl propionate in aquo-n- propanol media having varying concentration of n-propanol from 20 to 80% (v/v) at 5 different temperatures i.e. at 20, 25, 30, 35 and 40°C.

EXPERIMENTAL:

Export quality of butyl propionate made in USSR and extra pure ethanol of Merck Grade were used. The kinetics of the reaction was studied as usual[1-2] by keeping the strength of alkali 0.1 M and that of the ester(butyl propionate) 0.05 M in the reaction mixture. The reaction was found to obey the second order kinetic equation and the evaluated values of specific rate constants have been recorded in Table-I, From the recorded values of log k and 103/T, in Table - II, log k values were plotted against 103/T, The values of iso-composition activation energy (EC) and iso-dielectric activation energy (ED) have been mentioned in Table - III and IV respectively. The log k values were plotted against log [H2O] from their values recorded in Table - V, the evaluated values of the slopes of these plots have been noted in Table - VI. The consolidated values of the thermodynamic activation parameters, i.e. ΔH^*, ΔG^* and ΔS^* were calculated by using Wynne-Jones and Eyring[3] relation are enlisted in Table - VII.

Effect of Solvent on the Specific Rate Constant values of the Reaction :

From the survey of the data recorded in Table - I, it is obvious that the rate of the reaction decreases regularly with gradual addition of ethanol in the reaction media at all the temperatures at which the kinetics of the reaction has been studied. In order to study the variation in rate constant values with increasing concentration of ethanol in the reaction media, the log k values have been plotted against mol % of ethanol content in the reaction media as shown in Fig. - 1., Figure - 1 shows that the rate of reaction go on decreasing having different slopes due to two intersecting straight lines in the plots at

about 18.25 mol % of ethanol in the reaction media. From Fig. - 1, it is also apparent that with increase in temperature, the degree of depletion in the rate become shallow (slow). Such decrease in the rate with increasing proportion of the organic co-solvent like ethanol is not new, but a number of researchers like Laidler-Landskroener[4], Singh and Jha et al.[5] and Akanksha & Singh et al.[6] have also reported similar finding and their inferences about the depletion in rate with increasing concentration of the organic co-solvent in the aquo-ehtanol reaction media. Howerer, the possible rate depleting factors in the rate may be listed as follows:

(i) decrease in the bulk dielectric constant of the reaction media

(ii) decreasing the polarity of the reaction media on adding less polar ethanol

The above noted two rate depleting factors are quite in operation and this is in support of the earlier reports of Kumar, N[7] , Singh & Lal et.[8], and recent reoprt of Pathak & Singh et al[9] that the rate ought to decrease with decreasing dielectric constant value of the reaction media with addition of organic solvent to it. Thus, dielectric efect and solvation effect by the reaction media are responsible for depletion in the specific rate costants of the reacton.

Solvent Effect on the Iso-composition Activation Energy of the Reaction:

From the slopes of the Arrhenius plots of log k values against 103/T (from their values enlisted in Table - II) as shown in Fig.-2, the iso-composition activation energy (EC) of the reaction were evaluated and mentioned in Table - III.

From the values recorded in Table-III, it is obvious that EC or Eexp values go on increasing from 106.53 to 140.67 kJ/mol with increasing concentration of ethanol from 20 to 80% (v/v) in the reaction media. This trend is probably due to solvation changes taking place either at initial state level or at the transition state level or at the level of both the states as reported earlier by several researchers in this field. Considering the extent of solvation to be a dominant factor, the following three factore seem to be responisible for increase in EC values with gradual addition of ethanol in the reaction media -

(1) The initial state is less desolvated than the transition state,

(2) The initial state is more solvated than the transition state, and

(3) The transition state is desolvated and the initial state is solvated.

The transition state being smaller anion(ester + OH-) available less for ethanol molecule than the initial state, so the third factor seems to be operatiove in this case and it also gets support when the values of activation(ΔS^*) and enthalpy of activation (ΔH^*) go on increasing with increasing concentration of ethanol (Table-VII). Similar interpretation for enhancement in the values of Iso-composition activation energy of the reaction with gradual addition of the organic content in the reaction media have also been reported earlier by Singh & Singh et al.[10], Kumari1 & Singh et al.[11] and in recent years by Kishor & Singh et al.[12].

Effect of Solvent on the Iso-dielectric Acti tion Energy (ED) of the reaction:

On perusal of the data of Table - IV, it is observed that the iso-dielectric activation energy (ED) values of the reaction go on decreasing from 140.06 kJ/mol to 113.16 kJ/mol with increase in D values from D = 35 to D = 65 respectively. Such depletion in ED values with increase in D values of the reaction media are in accordance with the increase in EC values with increasing concentmition of the organic content (ethanol) in the reaction media. Since D values of the reaction media decreases with addition of organic solvent in it, so it can also be concluded that ED values of this reaction also increases like EC values with decrease in D values of the reaction media. However, these findings and interpretations regarding

change (decrease) in ED values with increase in D values of the reaction media are in support of the past views of Elsemongy[13] and Wolford[14] and have also been found in support of the recent report of Kumar & Singh et al.[15] and Rakesh & Singh et al[16].

Effect of number of water molecules of the reaction media in the Mechanism of the Reaction:

For establishing the mechanistic pathways of the reaction, Robertson et al.[17] gave an idea of solvation number 'n' which is the number or the number of water molecules involved in the formation of the activated complex and for its evaluation he proposed the equation:

$$\log k = \log k' + n \log [H2O]$$

Robertson et al[17] have established the principle that the values of solvation number (n) fo the reaction following unimolecular mechanistic pathway is fairy high but for the reaction following bimolecular path, it will be low. The number of water molecules 'n' involved in the formation of the activated complex of the reaction were determined by plotting log k values against log [H_2O] value for alkali catalysed hydrolysis of buthyl propionate in aquo-ethanol media. The value of log k and log [H_2O] have been tabulated in Table - V and their plots have been pictured in Fig - 3. The numerical values of the slopes of plots have been recorded in Table - VI. From Fig. - 3, it is clear that at each temperature of the reaction, the polts of log k versus log [H_2O], two intersecting straight lines having, different values of slopes are obtained at log [H_2O] value at about 1.49 which corresponds to 55.60% of water in aquo-ethanol media. From the values recorded in Table - VI, it is clear that below log [H_2O] value 1.490, which corresponds to 55.60% of water in the reaction media, the number of water molecules associated with the activated complex decreases from 0.827 to 0.343 with rise in temperature of the reaction from 20 to 40°C. Similarly, in case of above, 55.60% of water concentration in the reaction media, the values of slopes decreases from 1.535 to 0.641 with increase in temperature from 20 to 40°C of the reaction. Overall, it may be inferred that number of water molecules associated with the activated complex in its formation decreases from 1.535 to 0.343. In the light of guidelines of Robertson et al.[17] from the decreasing number of water molecules from 1.535 to 0.343 involved in the formation of the activated complex, it may be inferred that the mechanistic pathway followed by the reaction is changed from unimolecular to bimolecular in presence of ethanol in the reaction media and with increase in temperature of the reaction from 20 to 40°C. Regarding the changes in the structure of water, it is obvious that in presence of ethanol and with rise in temperature, water components of the reaction media, changes its structure from bulky to dense form.

$$(H_2O)_b \quad (H_2O)_d$$

Similar observations and inferences have also been reported earlier by Singh & Wats et al.[18] and recently by Rashmi & Singh et al.[19]

Solvent effect on Thermodynamic Activation Parameters of the Reaction:

For better study of the effects of solvent, the thermodynamic activation parameters, such as enthalpy of activation ΔH*, entropy of activation ΔS* and free energy of activation ΔG* were taken into account as they have great significance. These parameters evaluated using Wynne- Jones and Eyring3 quation have been recorded in Table -VII. In orderr to highlight the effect of solvent concentration on these thermodynamic paraneters more clearly, ΔH*,ΔG* and ΔS* values were plotted against mol % of ethanol as shown in Fig. - 4, 5 and 6 respectively. The values of ΔG* recorded in Table –VII obviously indicate that the variation in ΔG* is small and it increases from 87.11 to 89.42 kJ/mol with change of proportion of ethanol from 20 to 80% (v/v) at 30°C slowly with gradual addition of the organic content in water. The small but considerable increase increase in ΔG* and non-linear variation in ΔH* and ΔS*

curves with the increasing mol% of ethanol are indication of specific solvation taking place in the process of activation as already reorted by Elsemongy et al.[20], Saville & Hudson et al.[21] and Tomilla et al.$_{22}$ Simultaneous increase in ΔG*, ΔH* and ΔS* values with 148ropionate mol% of ethanol in the reaction media are only possible when the extent (degree) of enhancement in ΔH* values is greater than that in ΔS* values and from this, it may be inferred that in alkali catalysed hydrolysis of butyl 148ropionate aquo-ethanol media, ethanol acts as entropy controller and enthalpy stimulator solvent. Such inferences have been found in support of the earlier reported views of Monalisa & Singh et al.[23] and also of recently reported findings of Singh & Nazia et al.[25] and Priyanka & Singh et al.[25]

Obedience of Barclay-Butler Relationship and Solvent-solute Interactionin aquo-Ethanol media :

This reaction is found to obey Barclay-Butler[26] relationship as a straight line is obtained when ΔH* values are plotted against ΔS* at 30°C (values mentioned in Table - VII) as shown in Fig.- 7. From the value of the slope of the plot, the values of iso-kinetic temperature of the reaction comes to be 308.95 ≈ 309.0 . In the light of the reports of Leffler[27], high and considerable values of iso-kinetic temperature shows that in presence of ethanol, there is appreciably strong solvent-solute interaction in the reaction media (aquo-ethanol). Such observations and their interpretations have also been communicated earlier by Kumar & Singh et al.[28] and recently by Singh & Parween et al.[29].

REFERENCES

1. Ananthkrishnan, S.V. and Radhakrishnamurthi, R.S.: Indian J.Chem.3,336,1965

2. Singh, Lallan, Singh,R.T., Singh,,R. K. and Jha, R.C. : J. Indian Chem. Sco., 55, 372, 19

3. Wynne Jones W.F.K. and Eyring, H. : J. Chem. Phys., 3, 492, 1935

4. Laidler, K. J. and Landskroener, P. A. : Trans Faraday Soc., 1956, 52, 200 5.Singh,Lallan, Singh, R.T. and R.T. and Jha, R. C. : J.Indian Chem. Sco., 58, 966, 1981 6.Akanksha, Kumari, R., Kumar, R. and Singh,R.T. : ARJ Phys. Sci., 17, No.(1-2), 75-86, 2015 7.Kumar, N. : NIRJ Sci. 20, 51-64, 2016

8. Singh, R.T., Lal, V.K., Arya, N. and Singh,R.I. : ARJ Phy. Sci., 18, No. (1-2), 75-86, 2015

9. Pathak,S.N.,Radha,B.,Kumar,S. and Singh, R.T.: NIRJ Sci. 23,39-49, 2017(September)

10. Singh,H., Prasad, O.P., Ojha, R. and Singh, R.T. : NIRJ Sci. 20, 65-77, 2016(September) 11.Kumari, S., Kumari, M., Rai, C.L. and Singh R.T. : ARJ Phys. Sci., 18, No. (1-2), 61-73, 2015

12. Koshor, K., Kumari,A., Kumari,S. and Singh, R.T. : NIRJ Sci. 23, 39-49, 2017(September)

13. Elsemongy, M. M. :Z. Physik Chem. (Neue Folge), 1975, 94, 69 14. Wolford, R. K. : J. Phys. Chem., 68, 3392, 1964

15. Kumar, S., Kumar, N., Puja and Singh, R. T. : ARJ Phys. Sci., 18, No. (1-2), 87-99,2015 16.Kumar Rakesh and Singh, R.T : NIRJ Sci. 22, 39-51, 2016(Dec.)

17. Robertson, R.E., Heppolitile, R.L. and Scott, J.M.: Canad.J. Chem. Soc., 37, 803, 1959

18. Singh, R.T., Wats, K., Kumari, R. and Kaushalendra, K. : NIRJ Sci. 18, 33-43, 2015(Sept.)

19. Rashmi, Singh, V.K., singh, P. and Singh, R.T. : ARJ Phys. Sci., 19, No. (1-2), 75-87, 2016

20. Elsemongy, M.M. Abu Elamayam, M. S. and Moussa, M. N. H. : Z. Physik Chem.(Neue Folge), 1971, 75, 215

21. Saville, B. J. and Husdan, R.F.: J. Chem.Soc.,20,120,1955

22. Tomilla, E. and Mevikallio : Somun Kemi, 26C, 79, 1953

23. Monalia, Verma, S., Singh, D.K. and Singh, R.T. : NIRJ Sci. 17, 35-47, 2015

24. Singh, R., Nazia, S., K. Sweety and singh, R.I. : ARJ Phys. Sci, 19, No.(1-2), 93-102, 2016

25. Priyanks, K., Verma, S., Singh, H. and Singh, R.T. : NIRJ Sci. 22, 79-91, 2016(Dec.)

26. Barclay, I.M. and Butler, J.A.V. : Trans Faraday Soc., 34, 1445, 1938 27. Leffler, J.E. : J. Org. Chem., 20, 1201, 1955

28.Kumar,S., Kumar, N., Puja and Singh, R.T. : ARJ Phys. Sci., 18, No.(1-2), 87-99, 2015 29.Singh,R.I., Parween, Z., Lal, V.K. and Singh, R.T. : NIRJ Sci. 23, 65-78, 2017(September)

Table - I : Specific rate constant values of Alkali catalysed hydrolysis of Butyl nicotinate in water- EtOH media K × 10^2 in $(dm)^3$ mol^{-1} min^{-1}

Temp	% of EtOH(v/v)						
in °C	20%	30%	40%	50%	60%	70%	80%
20°C	87.04	68.32	53.18	47.18	37.05	29.53	22.29
25°C	177.75	148.32	128.44	106.88	91.64	72.09	56.65
30°C	365.43	303.46	268.91	238.89	209.89	173.74	146.15
35°C	710.56	630.38	580.23	536.91	468.92	419.86	353.67
40°C	1416.45	1313.71	1192.61	1135.27	1050.03	950.17	857.24

Table - II : Variation of log k values of the reaction with 10^3/T in water-EtOH media.

Temp in	103	3+log k values at different % of EtOH (V/V)						
°C	T	20%	30%	40%	50%	60%	70%	80%
20°C	3.413	1.9397	1.8346	1.7496	1.6738	1.5688	1.4703	1.3481
25°C	3.356	2.2498	2.1712	2.1087	2.0289	1.9621	1.8579	1.7532
30°C	3.3	2.5628	2.4821	2.4296	2.3782	2.322	2.2399	2.1648
35°C	3.247	2.8516	2.7996	0.7636	2.7299	2.6711	2.6231	2.5486
40°C	3.195	3.1512	3.1185	3.0765	3.0551	3.0212	2.9779	2.9331

Table - III : Evaluated values of Iso-composition Activation Energy (EC or Eexp) of the reaction in water-EtOH media.

% of EtOH(v/v)	**20%**	**30%**	**40%**	**50%**	**60%**	**70%**	**80%**
E_C value in kJ/mol	106.53	112.92	117.72	121.98	126.06	133.17	140.67

Table - IV : Evaluated values of Iso-Dielectric Activation Energy (ED) of the reaction at different desired 'D' values of the water-EtOH media.

D values	**D = 35**	**D = 40**	**D = 45**	**D = 50**	**D = 55**	**D = 60**	**D = 65**
E_D values in kJ/mol	140.06	133.35	129.78	125.38	120.08	115.85	113.16

Table - V : Variation of log k values of the reaction with log [H2O] values of water-EtOH system (media) at different temperatures.

% of	**% of**	**log**	**3 + log k values**				
EtOh (V/V)	**H_2O**	**[H_2O]**	**20°C**	**25°C**	**30°C**	**35°C**	**40°C**
20%	80%	1.6478	1.9397	2.2498	2.5628	2.8516	3.1512
30%	70%	1.5898	1.8346	2.1712	2.4821	2.7996	3.1185
40%	60%	1.5229	1.7496	2.1087	2.4296	2.7636	3.0765
50%	50%	1.4437	1.6738	2.0289	2.3782	2.7299	3.0551
60%	40%	1.3468	1.5688	1.9621	2.322	2.6711	3.0212
70%	30%	1.2218	1.4703	1.8579	2.2399	2.6231	2.9778
80%	20%	1.0458	1.3481	1.7532	2.1648	2.5486	2.9331

Table - VI : Values of the slopes of the plots of log k versus log [H2O] at different temperatures

Temperature	**Slope – I When log[H_2O] value is below 1.49**	**Slope – II when log[H_2O] value is above 1.49**
20°C	0.827	1.535
25°C	0.7	1.138
30°C	0.508	0.982
35°C	0.449	0.795
40°C	0.343	0.641

Table -VII Variation of ΔH*, ΔG* and ΔS* values of the reaction with mol % of EtOH in water- EtOH meida

% of EtOH (v/v)	Mol % of EtOH	?H* in kJ/mol	?G* in kJ/mol at 30°C	?S* in J/K/mol at 30°C
20%	7.17	104.54	87.11	51.53
30%	11.69	109.7	87.58	73.02
40%	17.07	115.47	87.88	91.66
50%	23.59	119.76	88.18	104.22
60%	31.06	125.7	88.51	122.76
70%	41.87	131.16	88.98	139.18
80%	55.85	137.99	89.42	160.31

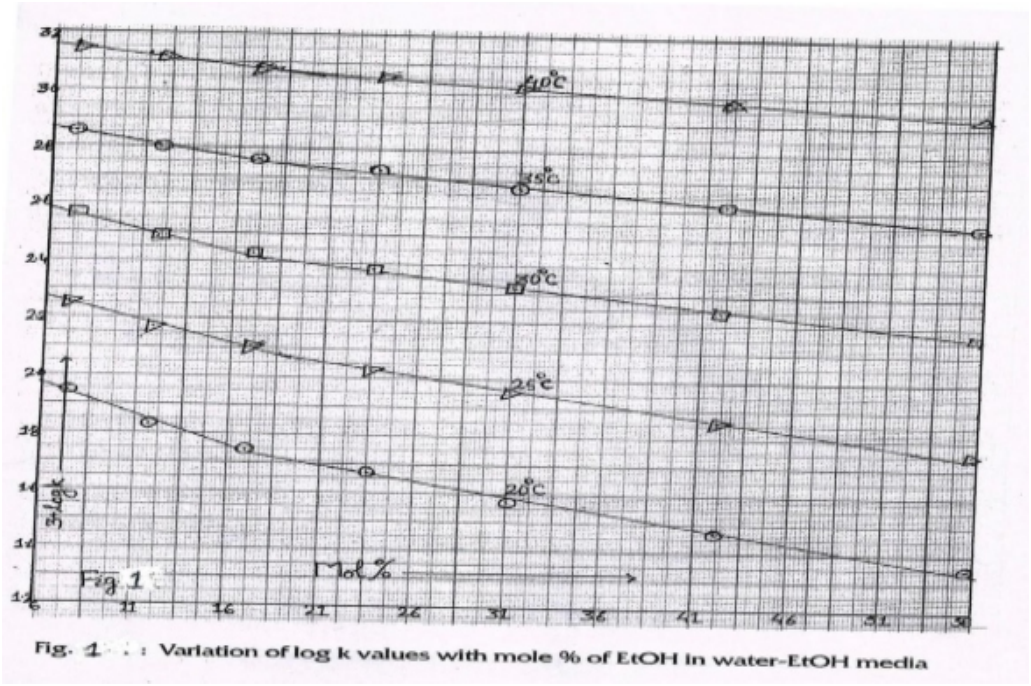

Fig. 1 : Variation of log k values with mole % of EtOH in water-EtOH media

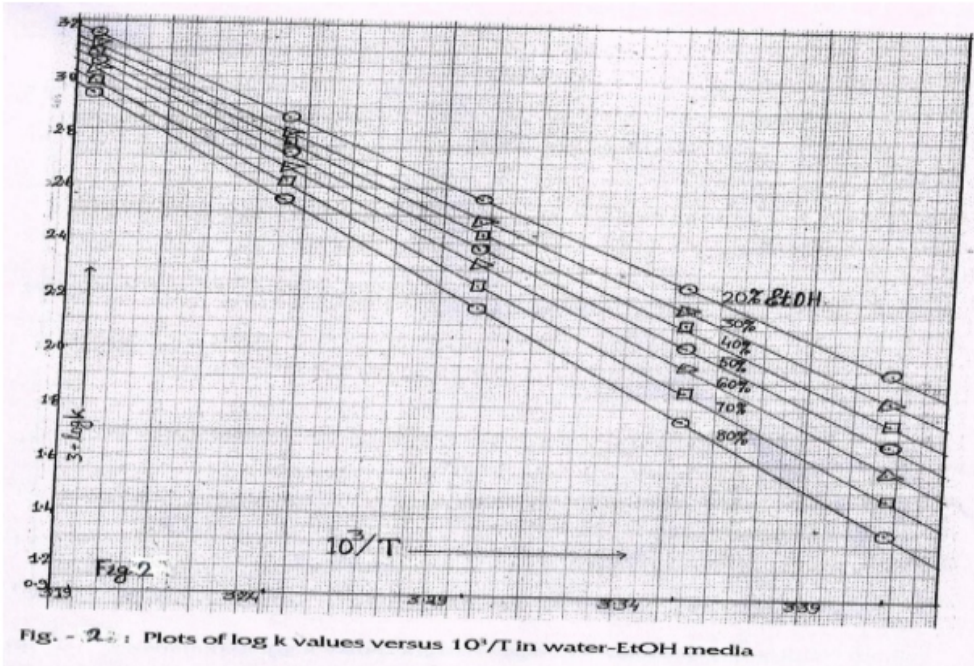

Fig. - 2 : Plots of log k values versus $10^3/T$ in water-EtOH media

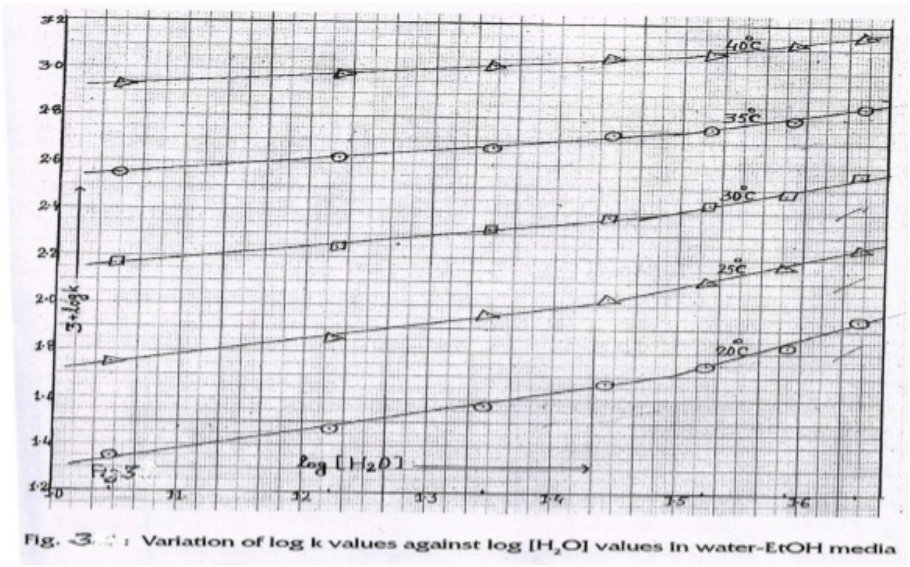

Fig. -3 : Variation of log k values against log [H_2O] values in water-EtOH media

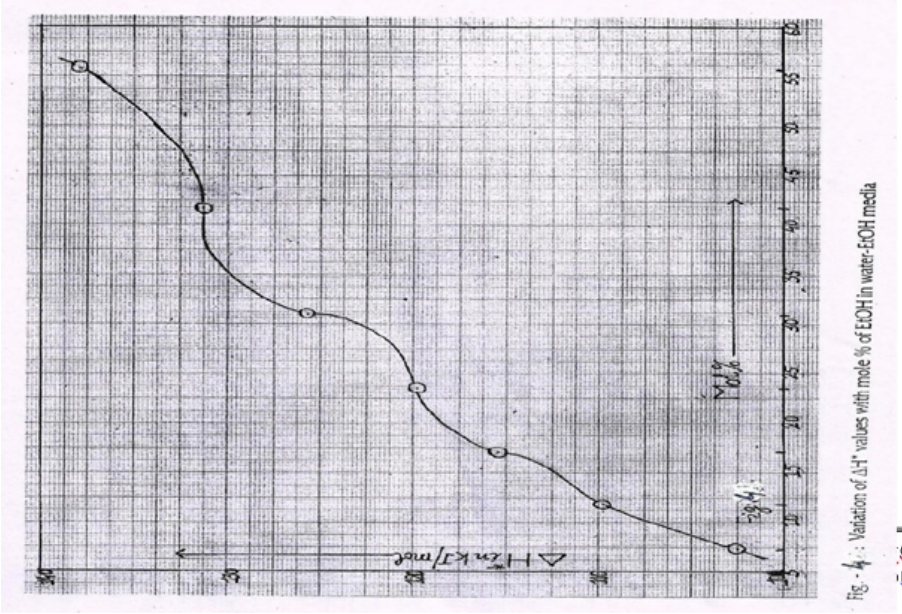

Fig. - 4 : Variation of ΔH^* values with mole % of EtOH in water-EtOH media

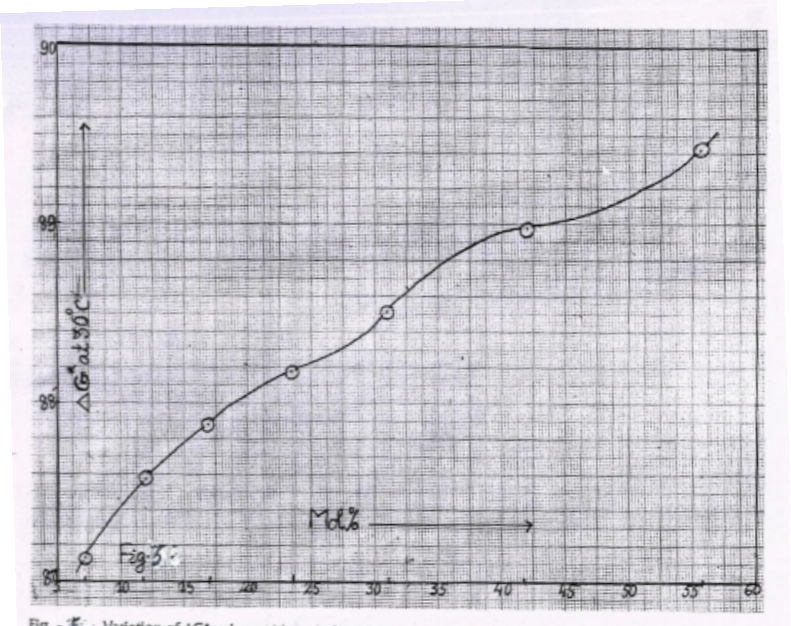

Fig. - 5 : Variation of ΔG^* values with mole % of EtOH in water-EtOH media

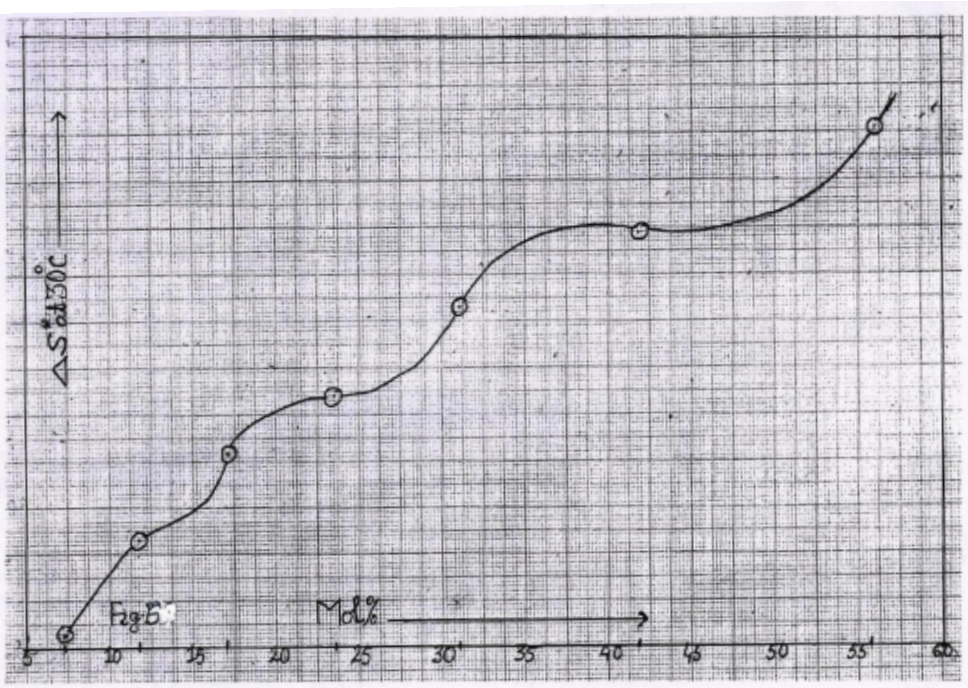

Fig. - 6 : Variation of ΔS* values with mole % of EtOH in water-EtOH media

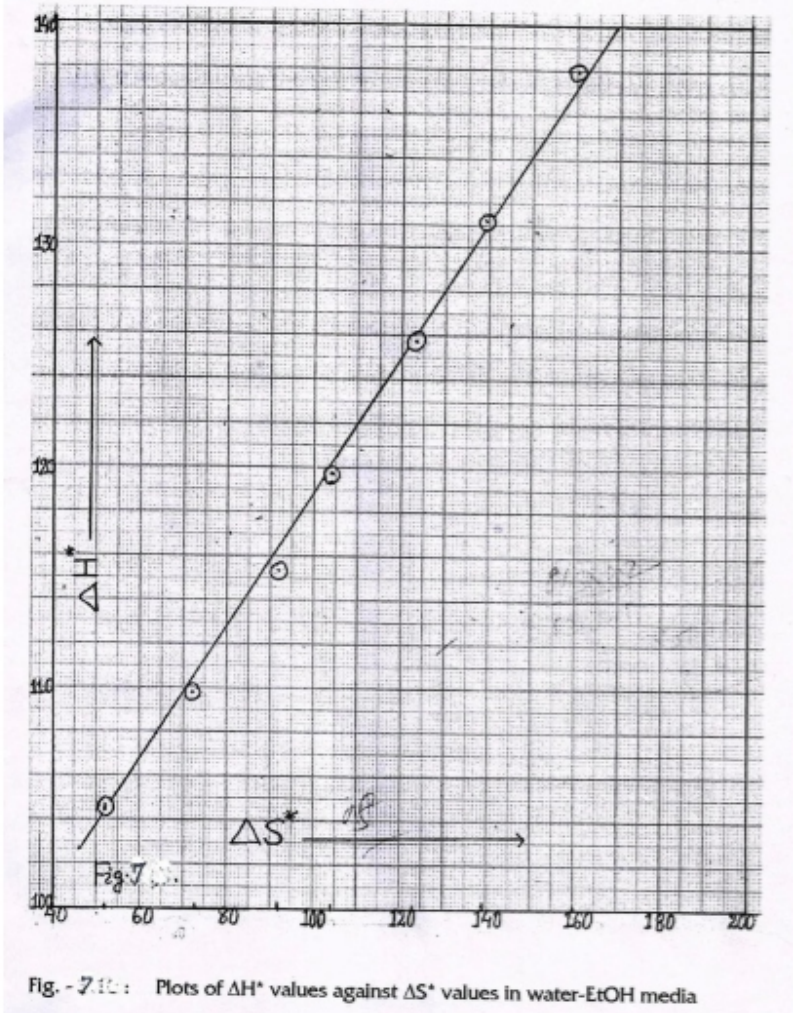

Fig. - 7 : Plots of ΔH* values against ΔS* values in water-EtOH media

Dielectric, Magnetic and Impedance Properties of BTBFT Multi Ferroic Ceramics

SHASHI PRAKASH RAI[1] AND [2]B. K MISHARA

[1.] Mansa Pandey Bag, Ara – 802301 , Bihar , India

[2.] Shreenath Niketan , Hazaribagh-825301 , Jharkhand , India

A B S T R A C T

The ternary bulk sample of (Bi0.8Tb0.1Ba0.1Fe0.9Ti0.1O3)was prepared by using a solid state reaction technique. In this paper the structural, electrical and magnetic properties of ceramics have been investigated. The XRD patterns of the samples at room temperature showed perovs kite phase with hexagonal structure at room temperature. Studies of dielectric properties of the compounds with frequency at different temperatures (25-400°C), exhibits two dielectric anomalies, one at 175oC and other around 320oC (ferroelectric–paraelectric type transition).The Curie temperature shifted towards the lower temperature with the increase in frequency. The low value of activation energy obtained for this ceramic samples could be attributed to the influence of electronic contribution to the conductivity. By using VSM technique, a significant change in the magnetic properties was observed for this ceramic. The highest magnetization field were found attemperature 5K. The impedance analysis confirm the non-Debye type behaviour of the compound.The relaxation frequency shifted to higher side with increase in temperature.The Nyquist plot and conductivity studies showed the NTCR character of samples.

Keywords: Ceramics; X-ray diffraction; Dielectric properties; Impedance spectroscopy; Magnetic property.

INTRODUCTION

From a technological point of view, the mutual control of electric and magnetic properties is an attractive possibility for recent research [1]. This offers potential applications for new devices of magnetic storage as well as ferroelectric devices. The perovskite type materials provide the vast spectrum of electrical properties covering ferroelectric-(anti-)ferroelectric, ferromagnetic-(anti-)ferromagnetic, metallic, and semiconductor. Hence the combination of these perovs kite materials opens various routes for achieving the multi ferroism properties in one phase material. Recently, several researcher reported on the synthesis and characterization of multi ferroic perovskite systems such as anti ferromagnetic- ferroelectric, weak ferromagnetic/anti ferromagnetic-ferroelectric and antiferro magnetic/weak ferromagnetic-ferroelectric systems [2, 3]. As a typical ferro electromagnetic material, $BiFeO_3$(BFO) is the most useful for practical application point of view owning to its high Curie (TC = 1103 K) and Neel (TN = 643 K) transition temperatures, and therefore it has attracted a great deal of research interest [4]. Because of the canting of the Fe sub lattice moment, $BiFeO_3$ shows a weak magnetic moment at room temperature [5]. The spontaneous magnetic moment was absent in pure $BiFeO_3$ up to 8 kOe because of the completely compensated anti ferromagnetic ordering[4]. Preparation of pure $BiFeO_3$ in the bulk ceramic form without traces of impurities has been a very difficult task. $BiFeO_3$-ABO_3solid solution systems have attracted great attention as a means to increase structural stability and sinter ability. Processing of BiFeO3 with other perovs kite structured materials, such as $BaTiO_3$, would prevent the formation of secondary phases [6, 7] and have excellent ferroelectric properties (TC= 120oC).The overall magnetic behaviors of bulk $ReFeO_3$ (Re-Rare Earth) are described as the result of two contributing magnetic 'sub lattices': (i) an anti ferromagnetic iron oxide lattice in which the spins are coupled via a Fe^{3+} - O^{2-} -Fe^{3+}super exchange mechanism; and (ii) a paramagnetic contribution from essentially non-coupled ions. Due to spin-canting in the iron containing sub lattice, a small ferromagnetic moment is observed as a result of the distorted perovs kite structure in one particular crystallographic direction[8]. Terbium ions (Tb^{3+}) possessing large atomic weight, smaller

size (Radius Tb^{3+} = 0.923 A°) as compared to Bi^{3+} Ions (Radius Bi^{3+} = 1.032 A°), comparable electroneg ativity with respect to Bi^{3+} ions, make Tb^{3+} ions the most suitable dopant[9-11]. Therefore, the large structural distortions would be expected by their substitutions in $BiFeO_3$. Moreover, Tb^{3+} ions possess large magnetic moment; upon their doping, the spiral modulated spin structure of $BiFeO_3$ could be partially destroyed and the spatial homogenization of spin arrangements could be realized[12, 13]. This results in the enhancement of the multi ferroic properties of the $BiFeO_3$, which is the motivation for the present study.In this study, the crystal structure, dielectric and magnetic properties of the perovskite system Bi0.8Tb0.1Ba0.1Fe0.9Ti0.1O_3 have been carried out to examine the behavior of the ceramic system. Tb and Ba were used to substitute at the A site of $BiFeO_3$, because their radii are similar, and they stabilize the perovs kite phase that helps to decreased Bi volatilization and the amount of oxygen vacancies. This system is a combination of three ternary perovs kite (two Ferromagnetic + one Ferroelectric) systems. The origin of the weak ferromagnetism has been discussed in terms of high temperature characteristics of this perovskite system. Electrical properties have been carried out by using complex impedance and modulus spectroscopy (CIS) technique[14], which is a very convenient tool to correlate the structural/microstructural and electrical properties relationship in a polycrystalline ceramics.

MATERIAL AND METHODS

Polycrystalline samples of (Bi0.8Tb0.1Ba0.1Fe0.9Ti0.1O_3) were synthesized from high purity oxides (Bi_2O_3 (99.9% pure M/S Aldrich chemicals USA), Fe_2O_3 (99.9% pure M/S Aldrich chemicals, USA), Tb_4O_7 (99.9% pure M/S Aldrich chemicals, USA), $BaCO_3$ (99.9% pure M/S Aldrich chemicals, USA) and TiO_2, (99.9% pure M/S Aldrich chemicals, USA), using solid-state reaction technique. The constituent compounds in suitable stoichiometric were thoroughly mixed in a ball milling unit for 42h. Then powder was dried at 125°C and calcined at 900°C for 4 h in alumina crucibles. The calcined fine powder was cold pressed into cylindrical pellets of 10 mm in diameter and 1-2 mm in thickness using a hydraulic press with a pressure of 50MPa. These pellets were sintered at a temperature i.e. 1000°C for 3 h. The formation and quality of compounds were verified with X-ray diffraction (XRD) technique. The XRD patterns of the compounds were recorded at room temperature using X- ray powder diffract to meter (Rigaku Minifiex, Japan) with CuKα radiation (λ = 1.5405 Å) in a wide range of Bragg angles 2θ (20° ≤ 2θ ≤ 60°) at a scanning rate of 2° min−1.Scanning Electron Micrographs (SEM) of the fractured surface of the specimen were obtained with a JEM-2000FX (JEOL Ltd.) scanning electron microscope operated at 25 kV.The flat polished surfaces of the sintered samples were electrode with air drying silver paste. Dielectric and impedance were determined by use of PSM1734 Impedance Analyzer at frequencies 1 kHz to 1MHz; samples were heated from room temperature to 400^0C.The magnetic data was recorded with the help of vibrating sample magnetometer (VSM) (Cryogenic).

RESULTS AND DISCUSSION STRUCTURAL STUDIES

Fig. 1 shows the XRD patterns of Bi0.8Tb0.1Ba0.1Fe0.9Ti0.1O_3 ceramics at room temperature. All patterns match with JCPDS#712494 data and shows that the samples have mixed phase with a hexagonalstructure at room temperature. All the reflection peaks were indexed using observed inter-planar spacing d and lattice parameters of Bi0.8Tb0.1Ba0.1Fe0.9Ti0.1O_3 with jcpds data base. The main peak of the samples are located at approximately 2θ = 31.84°, having hkl value <110>. Because of the kinetics of formation, the other impurity phases are obtained during synthesis. In my samples, the impurity phase was observed and it was shown as * in Fig. 1 and it may be attributed to $BaFe_2O_4$ (JCPDS#772337).

SEM images of sintered ceramic samples are shown in Fig. 2. It was observed that the grains are homogeneously distributed over the entire surface of the samples with less porosity. The grain sizes of the ceramic are in the range of 0.5-12μm. On the other hand, from the sintered ceramic surface (as-fired), homogeneous grains of various sizes can clearly be seen.

DIELECTRICS STUDIES

Fig. 3shows the variation of e and tanδ with temperature at frequencies 1 kHz-100 kHz for Bi0.8Tb0.1Ba0.1Fe0.9Ti0.1O3 (BTBFT) were obtained on silver electrode samples in plane capacitor configuration. The observed peaks in the dielectric constant can be correlated to the two phase transitions from ferroelectric to ferroelectric and ferroelectric to parael ectric at temperatures 175°C and 320°C respectively. These two peaks are due to two different ferroelectric compounds present in the ceramic system i.e. $BiFeO_3$ and $BaTiO_3$. With increase in temperature, the dielectric constant increases up to 170°C, and then decreases up to 235°C. After 235°C dielectric constant increases again up to 320°C. This is due to the presence of different types of polarizations (electronic, atomic, ionic, dipolar and space-charge) at low frequencies and high temperatures. As in normal ferroelectrics, the dielectric constant of and samples increases gradually with increasing temperature up to the transition temperature and thereafter it decreases with increasing temperature. BTBFT sample shows the maximum value of dielectric constant with transition temperatures for different frequencies (1 kHz-100 kHz) are shown in Table 1.We observed that the real and imaginary part of dielectric constant decrease with the increase in frequencyas shown in Fig. 4. The decrease in the dielectric constant (ε¢) can be explained on the basis of decrease in polarization with frequency. At low frequencies, all the polarizations respond easily to the time varying electric field but as the frequency of the electric field increases different polarization contributions filters out, as a result, the net polarization of the material decreases which leads to the decrease in the value of ε¢. Further, the decrease of ε¢¢with the increase in frequency can be explained by Debye formula [15]. At lower frequencies tan δ is inversely proportional to frequency which explains the decrease in tanδ with frequency. $Bi0.8Tb0.1Ba0.1Fe0.9Ti0.1O_3$ sample shows the maximum value of dielectric constant for different frequencies as shown in Table 1.

Fig. 5shows the variation of log ζac (s/m) vs 1/T (K-1) of $Bi0.8Tb0.1Ba0.1Fe0.9Ti0.1O_3$ ceramics at 1kHz -100 kHz frequencies in the temperature range from 325°C to 345°C. The ac electrical conductivity was calculated from the impedance data using the formula ζ = ωεεotanδ, where εo is the vacuum dielectric constant, ω is the angular frequency and kB is the Boltzmann constant. The value of activation energy was calculated in the paraelectric region from the plot of ln(ζac) vs 1/T using the conductivity relation $\zeta = \zeta^{o} \exp(-Ea/kBT)$[16]asshown in Table 1.It is observed that σac increase with increasing temperature which confirming the NTCR behaviour. At high temperature, the donor cations have a major part to play in the conduction process and activated with small energy which is called activation energy. The activation energy for all composition at different frequency was found to be very low in the paraelectric region. This may be due to ionic solids having a limited number of mobile ions being trapped in relatively stable potential wells during their motion through the solid. Due to a rise in temperature the donor cations are taking a major part in the conduction process. The donors have created a level (i.e. band-donor level), which is much nearer to the conduction band. Therefore, only a small amount of energy is required to activate the donors. In addition to this, a slight change in stoichiometry in multi-metal complex oxides causes the creation of large number of donors or acceptors, which creates donor or acceptors like states in the vicinity of conduction or valance bands. These donors or acceptors may also be activated with small energy[17].

Electrical studies.

The electrical properties of $Bi0.8Tb0.1Ba0.1Fe0.9Ti0.1O_3$ ceramics were investigated by the help of complex impedance spectroscopy (CIS) technique. It is important to transform the dielectric and electrical data in different formalism and analyze them to get true picture of the material. The use of function Z* and Y* is particularly appropriate for the resistive and/or conductive analysis where the long-range conduction dominates, whereas the ε* and M* functions are suitable when localized relaxation dominates. So the plotting of ac data in terms of impedance, electric modulus, and dielectric permittivity simultaneously gives a complete assignment of all the physical processes taking place in the material.

The variation of real part of impedance (Z′) with frequency at various temperatures (from 225 to 325 °C) for $Bi0.8Tb0.1Ba0.1Fe0.9Ti0.1O_3$ ceramics is shown in Fig. 6. The pattern shows a sigmoid variation as a function of frequency in the low frequency region followed by a saturation region in the high frequency region. This suggests the presence of mixed nature of polarization behavior in the material, such as electronic, dipolar and orientation polarization. A decreasing trend of Z′ with rise in temperature suggests the presence of negative temperature coefficient of resistance (NTCR) in the material in the low frequency region but tends to merge in the high frequency region at almost all temperatures. A possibility of increase in ac conduction (ζac) in the sample was observed due to the decrease in the magnitude of Z′ with rise in temperature. This increase in ac conduction with temperature may be due to the contribution of defects like oxygen vacancies. Generally, the contribution due to oxygen vacancies is more prominent in perovs kite structures at higher temperatures. These results indicate increase in ac conductivity with rise in temperature in the high frequency region (possibly) due to the release of space charge and lowering in the barrier properties of the material.

Fig. 7 presents the variation of imaginary part of impedance (Z″) as a function of frequency at different set of temperatures (from 225 to 325 °C) for $Bi0.8Tb0.1Ba0.1Fe0.9Ti0.1O_3$. With the increase of frequency, imaginary part of impedance (Z″) increases initially, attains a peak (Z″max) and then decreases with frequency at all measured temperatures. At higher frequency side all the curves are merged which might be due to the reduction in space charge polarization at higher frequency. The peak shifts towards higher frequency side with increasing temperature showing that the resistance of the bulk material is decreasing. Also,the magnitude of Z″ decreases with increasing temperature. This would imply that dielectric relaxation is temperature dependent, and there is apparently not a single relaxation time.

Fig. 8(a) shows the temperature-dependent spectra (Nyquist plot) of $Bi0.8Tb0.1Ba0.1Fe0.9Ti0.1O_3$ materials. By impedance spectrum we got the semicircular arcs at the set of higher temperatures. The nature of variation of the arcs with temperature and frequency provides various clues of the materials. However, as the temperature increased the slope decreased and found to curve towards the major (Z′) axis forming clear semicircular arcs. The radius of curvature was found to decrease with increasing temperature, which indicates the increase in conductivity of the sample with temperature. Generally, existence of a single semicircular arc represents only one contribution e.g. grain interior (bulk) property of the material. However, in the present case, the spectrum comprises of suppressed semicircular arcs indicating two different contributions from the grain interior (bulk) and grain boundary. The observed semicircular arcs have their centers lying off the real (Z') axis which is an indication of non-Debye type relaxation with a distribution of relaxation times instead of a single relaxation process. In general, the relaxation time for grain boundary region is much larger than that for the grains and, therefore, its

response relaxes at lower frequencies. Thus, the low frequency arc in the Nyquist plot corresponds to the grain boundary effects and the smaller high frequency arc to the grain/bulk effect of the material. In the other words the semicircular arc with the real axis (Z′) gives us an estimate of the bulk resistance (Rb) of the material. It has been observed that the bulk resistance of the material decreases with increase in temperature showing a typical semiconducting property, i.e. negative temperature coefficient of resistance (NTCR) behavior. The fitting of Nyquist plot for $Bi0.8Tb0.1Ba0.1Fe0.9Ti0.1O_3$ ceramics shown in Fig. 8(b)and it observed that with the increase in temperature the slope of the lines decrease and the lines bend towards real (Z′) axis and at higher temperatures (250°C, 275°C, 300°C and 325°C); a semicircle could be traced, indicating the increase in conductivity of the sample. It can also be observed that the peak maxima of the plots decrease and the frequency for the maximum shifts to higher values with the increase in temperature. It can be noticed that the complex impedance plots are not represented by full semicircle, rather the semicircular arc is depressed and the centre of the arc lies below the real (Z′) axis suggesting the relaxation to be of poly dispersive non-Debye type in samples. This may be due to the presence of distributed elements in the materialelectrode system.[14, 18]. An equivalent circuit is being used to provide a complete picture of the system and establish the structural property relationship of the materials. Comparison of complex impedance plots (symbols) with fitted data (lines) using commercially available software ZSimpwin Version. To model the non-Debye response, constant phase element (CPE) is used in addition to resistors and capacitors. Here it has also been clearly observed from the Nyquist plots that the influence of grain size on the inter grain resistivity increases with decreasing grain size.

Fig.9 shows the variation of real part of electric modulus (M′) with frequency at higher temperatures between 250°C-325°Cfor $Bi0.8Tb0.1Ba0.1Fe0.9Ti0.1O_3$ ceramics. It is characterized by a low value of M′ in the low frequency region followed by a continuous dispersion with increase in frequency. It was found that M′ values saturated to a maximum (M_∞ - the asymptotic value of M′ at higher frequencies) in the high frequency region for all temperatures. The asymmetric plot of M′ is because of the stretched exponential character of relaxation time of the material. Monotonous dispersion on increasing frequency at lower temperatures may be caused by short range mobility of charge carriers. Such results may possibly be related to a lack of restoring force governing the mobility of the charge carriers under the action of an induced electric field. The value of M′ decreases with rise in temperature in the observed frequency range.

Fig. 10 shows the variation of imaginary part of electric modulus (M″) with frequency at higher temperatures for $Bi0.8Tb0.1Ba0.1Fe0.9Ti0.1O_3$ ceramics. By these graphs we found that the position of the peak M″max shifted to higher frequencies as the temperature was increased. Physically, the peak in the imaginary part of the electric modulus defines the regions where the carrier can move at long distances. At frequency above peak maximum, the carriers are confined to potential wells, being mobile on short distances. The peaks are asymmetric and broader than the ideal Debye curve. Also, a peak in the M″ imaginary part indicates a dielectric relaxation process in the solid, and the frequency to the maximum indicates the mean relaxation time of this process. As can be seen, the imaginary part of the electric modulus exhibits a very well defined peak. The frequency range where the peaks occur is indicative of transition from long range to short range mobility[19, 20]. Two peaks in graph confirms the co-existence of two systems.The complex electric modulus spectrum M′ versus M″ is shown in Fig. 11for all the samples at different temperatures. Two arcs are clearly observed over the entire measured frequency range in both the samples. In fact, the first arc is the contribution of grain boundaries whereas the second arc is the contribution of grains. The patterns are characterized by the presence of little asymmetric and depressed semicircular arcs whose centre does not lie on M′ axis. The behavior of

electric modulus spectrum is suggestive of the temperature dependent hopping type of mechanism for electric conduction (charge transport) in the system and non-Debye type dielectric relaxation. In a relaxation system, one can determine the probable relaxation time (s) from the position of the loss peak in the Z″ as well as M″ vs. log f plots according to the relation: $t = 1/\omega = 1/2\pi f$(f is the relaxation frequency). We found that the double semicircular arcs in the complex modulus plots with a small semicircle at high frequency and a large semi-circular arc in the low frequency region at the temperatures range(300°C - 375°C as shown in the Fig 11. The modulus spectrum shows a marked change in the shape with rise in temperature suggesting a probable change in the capacitance value as a function of temperature.

Fig. 12 shows the scaling behaviour of the sample was studied by plotting the normalized plot of M″/M″max and Z″/Z″max as a function of the normalized frequency at different temperatures for $Bi0.8Tb0.1Ba0.1Fe0.9Ti0.1O_3$ ceramics. The normalized plot overlaps on a single master curve at different temperatures. The modulus scaling behaviour gives an insight into the dielectric processes occurring inside the material [21]. The value of FWHM evaluated from the normalized spectrum is greater than $\log 2+\sqrt{3}$, and this indicates about non- $2-\sqrt{3}$ Debye type behavior which is well supported by complex impedance plot. The peaks shifts and broadening was observed at higher frequencies with increasing temperature. The appearance of temperature dependent peaks (Z″max and M″max) at a characteristic frequency ($\omega max=2\pi fmax$) indicates the presence of relaxation process, which is temperature dependent [22]. These relaxation processes may be due to the presence of immobile species at low temperature and defects which became mobile at high temperature.

The frequency spectra of the ac conductivity for the samples at different measuring temperatures are shown in Fig. 13. The frequency dependent conductivity can be described by the equation:

$$\zeta ac\ (\omega) = \zeta dc + A\omega n \qquad (1)$$

Where n is the frequency exponent in the range of $0 < n < 1$. A and n are thermally activated quantities, hence electrical conduction is a thermally activated process. The frequency at which change in slope takes place is known as hopping frequency. At higher frequency, the hopping takes place by charge carriers through trap sites separated by energy barriers of varied heights. The number of charge carriers which have high relaxation time due to higher energy barriers and respond in low frequency region might be less in numbers and so the conductivity is lower at low frequencies. While the more charge carriers are with low barrier heights and these charge carriers easily respond with the frequency and at higher frequency they showed higher conductivity. The thermal energy of the charge carriers was increased at higher temperatures and so the potential height was also reduced. The conductivity spectrum shows a low frequency dispersion region followed by a high frequency plateau region. The low frequency region has been attributed to the ac-conductivity whereas the frequency independent plateau region corresponds to the dc conductivity. The dispersion behaviour may be due to presence of space charge while in the plateau region space charge vanishes. It is reasonable since the space charge vanishes at higher frequency domain. At lower temperatures ζac linearly varies with frequency and nonlinearity occurs in the high frequency region. This behaviour suggests that the hopping mechanism might be playing an important role in conduction process in the low temperature region.

MAGNETIC STUDIES

Fig. 14 shows the magnetic hysteresis loops measured at 5K, 10K, 150K and 300 K. The magnetization curves of the loop at low field are not collinear and this shows a weak ferromagnetic nature of samples, which could be further confirmed by the nonzero remnant magnetization and coercivity as shown in the

partly enlarged curves in the inset of Fig. 14. The highest magnetization, coercive field and M-H loop area were found for 5K. The enhancement of magnetization in this sample is always ascribed to the size effects of the suppression of helical order, i.e., incomplete rotation of the spins along the direction of the wave vector, increasing in spin canting due to surface strain and oxygen defects [23, 24]. On the other hand, oxygen defects could also enhance the magnetization by introducing Fe^{2+} into the ferromagnetic order across Fe^{3+}- O^{2-} - Fe^{2+} [23, 25].Furthermore, during the high temperature annealing process, the canting angles in samples were further modulated by theinteraction between the external magnetic field and the uncompensated spins in the canted anti ferromagnetic order, which may be the major reason causing the net magnetization to increase.

The magnetic moment as a function of temperature between 5 and 300 K under zero- field cooled (ZFC) and field cooled (FC) conditions with an applied magnetic field of 0.1 T is given inFig. 15. The magnetic moment (M) vs. temperature (T) curves of $Bi0.8Tb0.1Ba0.1Fe0.9Ti0.1O_3$ sample under the ZFC and FC conditions present a systematic change. The high magnetization value at the lower temperature suggests the presence of uncompensated anti ferromagnetic spins (Fe^{3+})[26]. Initially magnetization decreases with an increase in temperature, and then increases as shown in Fig. 15.As temperature goes down further from 300 to 5 K, the magnetization increases rapidly, confirming that there is a magnetic phase transition. The magnetic phase transition is suggested to be a transformation of Fe sub lattice from anti- ferromagnetic to weak ferromagnetic at low temperature [27]. The variation of M–T curves with $Bi0.8Tb0.1Ba0.1Fe0.9Ti0.1O_3$ sample may be attributed to different factors like (i) variation in the oxygen stoichiometric and doping at A and B sites, (ii) reduction in particle size and (iii) change in the magnetic anisotropy[28].The saturation of magnetization is not reached for all studied samples even with an applied magnetic field up to 10 T.

CONCLUSIONS

$Bi0.8Tb0.1Ba0.1Fe0.9Ti0.1O_3$ (BTBFT) solid solution ceramic was prepared using solid state reaction method. BTBFT ceramics were investigated for its dielectric properties by Impedance Spectroscopy (IS) in the temperature range of RT-500_oC and in the frequency range of 100 Hz -1 MHz. Studies of temperature dependent dielectric properties of sample exhibits two dielectric anomalies one at 175oC and other around 320°C.Curie temperatures320°C-310°C and exhibiting a hexagonal crystal system and Tc decreased with frequency. In case of magnetization, the coercive field was found to be decreased with temperature 5K, 10K, 150K and 300K.A minor loop traced for all these samples indicates an anti ferromagnetic nature with weak ferromagnetism. Real and imaginary parts of complex impedance and modulus properties of the materials were investigated by using complex impedance spectroscopy (CIS) technique. At a higher temperatures, the observed double semicircles in electric modulus plots confirms about the formation of samples in single phaseand indicates the presence of both bulk and grain boundary contributions. Impedance analysis indicates the presence of mostly bulk (grain) resistive contributions in the materials at higher temperatures whereas complex modulus plots shows the presence of grains as well as grain boundary contributions in the materials. It is due to the fact that impedance plot highlights the phenomenon with largest resistance whereas electric modulus plot highlights the phenomenon with smallest capacitance. Due to the large difference between resistive values of grains and grain boundaries, it is not possible to get two semicircles on the same impedance plot. Both impedance and modulus analysis support the typical behavior of negative temperature coefficient of resistance (NTCR) of the materials. They also confirm the presence of non-Debye type of relaxation phenomenon in the materials.

REFERENCES

[1] VE Wood, A Austin (1974) Austin, Possible applications for magnetoelectric materials. Int. J. Magn 5: 303.

[2] JS Kim, CI Cheon, PW Jang, YN Choi, CH Lee (2004) Ferroelectric and ferromagnetic properties of $0.2BiFeO_3$-$0.2RFeO_3$-$0.6ATiO_3$(R= Pr, Nd and A= Ba, Pb) and $0.8BiFeO_3$-$0.2BaTiO_3$. Journal of the European Ceramic Society 24: 1551.

[3] JS Kim, CI Cheon, CH Lee, PW Jang (2004) Weak ferromagnetism in the ferroelectric $BiFeO_3$ –$ReFeO_3$–$BaTiO_3$ solid solutions (Re= Dy, La). Journal of applied physics 96: 468.

[4] J Wang, JB Neaton, H Zheng, et al. (2003) Epitaxial $BiFeO_3$ Multiferroic Thin Film Hetero structures. Science 299: 1719. Doi:10.1126/science.1080615

[5] F Chang, N Zhang, F Yang, S Wang, G Song (2007) Effect of Cr substitution on the structure and electrical properties of $BiFeO_3$ ceramics. Journal of Physics D: Applied Physics 40: 7799.

[6] M Mahesh Kumar, A Srinivas, S Suryanarayana (2000) Structure property relations in BiFeO3/BaTiO3 solid solutions. Journal of applied physics 87: 855.

[7] MT Buscaglia, L Mitoseriu, V Buscaglia, et al. (2006) Preparation and characterisation of the magneto-electric< i> x</i> BiFeO< sub> 3</sub>–(1−< i> x</i>) BaTiO< sub> 3</sub> ceramics. Journal of the European Ceramic Society 26: 3027.

[8] R Rai, I Bdikin, MA Valente, AL Kholkin (2010) Ferroelectric and ferromagnetic properties of Gd-doped BiFeO< sub> 3</sub>–BaTiO< sub> 3</sub> solid solution. Materials Chemistry and Physics 119: 539.

[9] R Kiyanagi, T Yamazaki, Y Sakamoto, et al. (2012) Structural and Magnetic Phase Determination of (1-x) $BiFeO_3$–x $BaTiO_3$ Solid Solution. Journal of the Physical Society of Japan 81(2).

[10] SO Leontsev, RE Eitel (2009) Dielectric and Piezoelectric Properties in Mn-Modified (1− x) $BiFeO_3$ –$xBaTiO_3$ Ceramics. Journal of the American Ceramic Society 92: 2957.

[11] R Melgarejo, M Tomar, R Guzman, S Singh (2005) Synthesis and Structural Characterization of $BiFeO_3$–$BaTiO_3$ Materials. Ferroelectrics 324: 101.

[12] Y-j Zhang, H-g Zhang, J-h Yin, et al. (2010) Structural and magnetic properties in Bi< sub> 1− x</sub>< i> R</i>< sub> x</sub> FeO< sub> 3</sub>(< i> x</i>= 0– 1,< i> R</i>= La, Nd, Sm, Eu and Tb) polycrystalline ceramics. Journal of Magnetism and Magnetic Materials 322: 2251.

[13] J Liu, L Fang, F Zheng, S Ju, M Shen (2009) Enhancement of magnetization in Eu doped $BiFeO_3$ nanoparticles. Applied Physics Letters 95: 022511.

[14] JR Mcdonald (1987) Impedance spectroscopy: emphasizing solid materials and systems. A Wiley-Interscience Publication, John Wiley & Sons, New York.

[15] H Birey (1978) Dielectric properties of aluminum oxide films. Journal of applied physics 49: 2898.

[16] P Uniyal, KL Yadav (2009) Observation of the room temperature magnetoelectric effect in Dy doped BiFeO 3. Journal of Physics: Condensed Matter 21: 012205.

[17] L Shu, X Wei, L Jin, Y Li, H Wang, X Yao (2013) Enhanced direct flexoelectricity in paraelectric phase of Ba(Ti[sub 0.87]Sn[sub 0.13])O[sub 3] ceramics. Applied Physics Letters 102: 152904.

[18] Dk Sharma, R Kumar, R Rai, S Sharma, Al Kholkin (2012) Impedance and modulus spectroscopy characterization of sodium-bismuth titanate-based lead-free ferroelectric materials. Journal of Advanced Dielectrics 2.

[19] R Rai, I Coondoo, R Rani, I Bdikin, S Sharma, AL Kholkin (2013) Impedance spectroscopy and piezoresponse force microscopy analysis of lead-free (1−< i> x</i>)K< sub> 0.5</sub> Na< sub> 0.5</sub> NbO< sub> 3</sub>−< i> x</i> LiNbO< sub> 3</sub> ceramics. Current Applied Physics 13: 430.

[20] A Shukla, R Choudhary, A Thakur (2009) Thermal, structural and complex impedance analysis of Mn< sup> 4+</sup> modified BaTiO< sub> 3</sub> electroceramic. Journal of Physics and Chemistry of Solids 70: 1401.

[21] P Das, P Chakraborty, B Behera, R Choudhary (2007) Electrical properties of Li< sub> 2</sub> BiV< sub> 5</sub> O< sub> 15</sub> ceramics. Physica B: Condensed Matter 395: 98.

[22] K Prasad, K Kumari, K Chandra, K Yadav, S Sen (2009) Dielectric relaxation and ac conductivity of WO3 added (Na1/2Bi1/2) TiO3 ceramic. Materials Science-Poland 27: 373.

[23] T-J Park, GC Papaefthymiou, AJ Viescas, AR Moodenbaugh, SS Wong (2007) Size- Dependent Magnetic properties of Single-Crystalline Multiferroic BiFeO3 Nanoparticles. Nano Letters 7: 766.

[24] D Kothari, VR Reddy, A Gupta, et al. (2007) Multiferroic properties of polycrystalline Bi1−xCaxFeO3. Applied Physics Letters 91.

[25] W Eerenstein, FD Morrison, J Dho, MG Blamire, JF Scott, ND Mathur (2005) Comment on "Epitaxial BiFeO3 Multiferroic Thin Film Heterostructures". Science 307: 1203.

[26] I Sosnowska, TP Neumaier, E Steichele (1982) Spiral magnetic ordering in bismuth ferrite. Journal of Physics C: Solid State Physics 15: 4835.

[27] S Zhang, M Lu, D Wu, Y Chen, N Ming (2005) Larger polarization and weak ferromagnetism in quenched $BiFeO_3$ ceramics with a distorted rhombohedral crystal structure. Applied Physics Letters 87: 262907.
[28] RK Mishra, DK Pradhan, RNP Choudhary, A Banerjee (2008) Effect of yttrium on improvement of dielectric properties and magnetic switching behavior in BiFeO3. Journal of Physics: Condensed Matter 20: 045218.Figure captions:

Table 1: Details of the physical parameters of Bi0.8Tb 0.1 Ba 0.1Fe0.9Ti0.1O3 ceramics. Fig. 1. XRD patterns of the Bi0.8Tb 0.1Ba 0.1Fe0.9Ti0.1O3ceramics.
Fig. 2. SEM micrographs of surface of the Bi0.8Tb0.1Ba0.1Fe0.9Ti0.1O3ceramics.
Fig. 3. Variation of real part of permittivity (ε′) as function of temperature of Bi0.8Tb0.1Ba0.1Fe0.9Ti0. 1O3ceramicsat different frequencies (1kHz-100 kHz).
Fig. 4. Variation of real and imaginary part of (ε¢ and ε¢¢) dielectric constant as a function of frequency of Bi0.8Tb0.1Ba0.1Fe0.9Ti0.1O3ceramics at different temperatures.
Fig. 5.Variation of ac conductivity (lnσac) as a function of absolute temperature (1/T) forBi0.8Tb 0.1Ba 0.1Fe0.9Ti0.1O3ceramics at different frequencies(1kHz-100kHz).
Fig. 6. Variation of real part of modulus (Z′) with frequency at different temperatures of Bi0.8Tb 0.1Ba0.1Fe0.9Ti0.1O3ceramics.
Fig. 7. Variation of imaginary part of modulus (Z″) with frequency at different temperatures of Bi0.8 Tb 0.1Ba0.1Fe0.9Ti0.1O3ceramics.
Fig. 8 (a)Variation of real and imaginary part (Z′ and Z″) ofimpedance and (b) Fitted graph of real and imaginary part ((Z′ andZ″) of impedance with different temperatures of Bi0.8Tb0.1Ba0.1Fe0.9Ti0.1O 3ceramics.
Fig. 9. Variation of real part modulus (M′) with frequency at different temperatures of Bi0.8Tb0.1Ba0.1 Fe0.9Ti0.1O3ceramics.
Fig. 10. Variation of imaginary part modulus (M″) with frequency at different temperatures of Bi0.8 Tb 0.1Ba0.1Fe0.9Ti0.1O3ceramics.
Fig. 11. Variation of real (M′) and imaginary part (M″) of modulus with different temperatures of Bi0.8 Tb 0.1Ba0.1Fe0.9Ti0.1O3ceramics.
Fig. 12. Scaling behavior of (Z″/Z′max) and (M″/M″max) vs. log (f/fmax) of Bi0.8Tb0.1Ba0.1Fe0.9 Ti0.1O3ceramics.
Fig. 13. Variation of lnσac (W/cm-1) vs. frequency of Bi0.8Tb0.1Ba0.1Fe0.9Ti0.1O3 ceramics at different temperatures.
Fig.14. M–H loops of Bi0.8 Tb 0.1Ba 0.1Fe0.9Ti0.1O3ceramics at (a) 5K, 10Kand(b) 150K, 300 K.
Fig.15. Variation of magnetic moment with temperature of Bi0.8Tb0.1Ba0.1Fe0.9Ti0.1O3ceramics for FC and ZFC.

Table 1: Details of the physical parameters of $Bi_{0.8}$ Tb $_{0.1}$ Ba $_{0.1}Fe_{0.9}Ti_{0.1}O_3$ ceramics.

Sample Name	***Freq.***	$T_{FE\text{-}FE}(^oC)$	ε_{max} ***(FE-FE)***	$T_{FE\text{-}PE}(^oC)$	ε_{max} ***(FE-PE)***	E_a ***(eV)***
$Bi_{0.8}Tb_{0.1}Ba_{0.1}Fe_{0.9}Ti_{0.1}O_3$	*1kHz*	*175*	*7298*	*315*	*2338*	*1.46*
	10kHz	*170*	*2101*	*320*	*920*	*1.37*
	100kHz	*170*	*722*	*310*	*384.5*	*1.06*

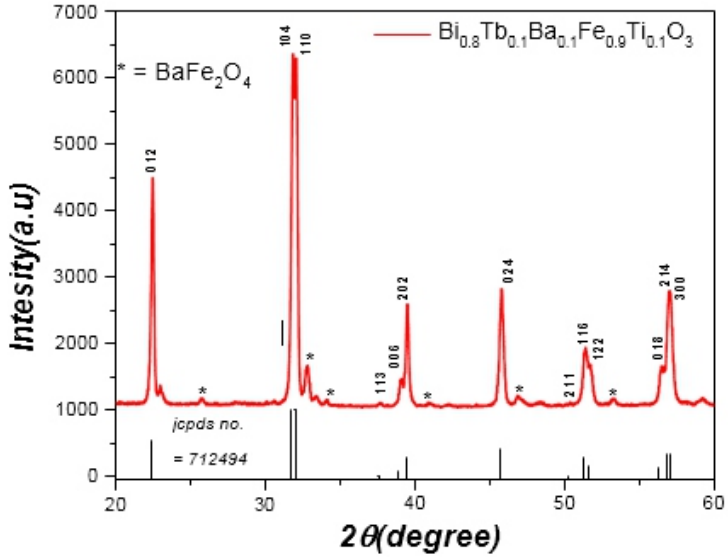

Fig. 1. XRD patterns of the Bi0.8Tb 0.1Ba 0.1Fe0.9Ti0.1O_3ceramics.

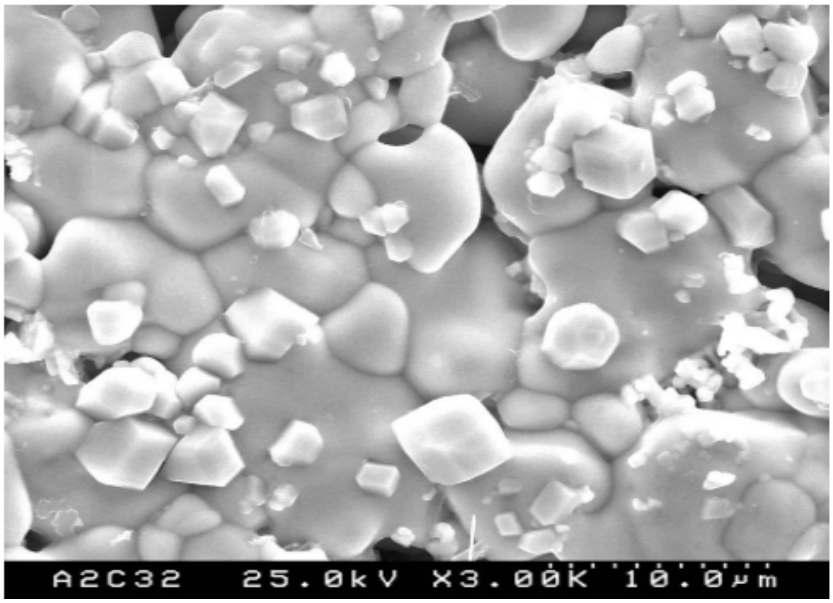

Fig. 2. SEM micrographs of surface of the Bi0.8Tb0.1Ba0.1Fe0.9Ti0.1O_3ceramics.

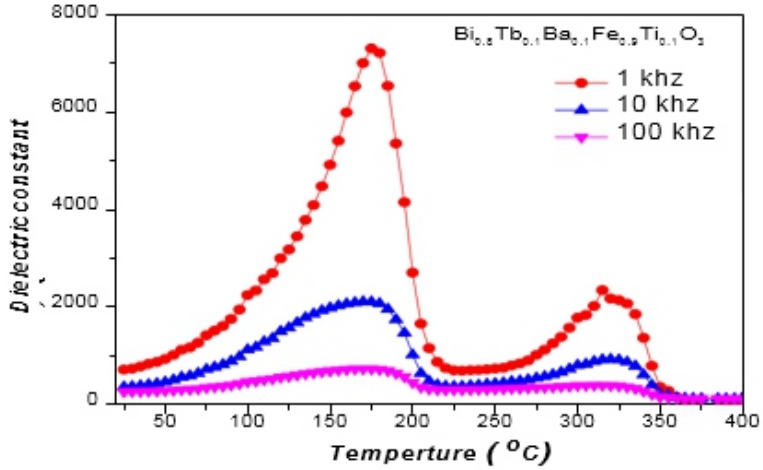

Fig. 3. Variation of dielectric constant (ε′) as function of temperature of Bi0.8Tb0.1Ba0.1Fe0.9Ti0.1O_3 ceramicsatdifferent frequencies (1kHz-100kHz).

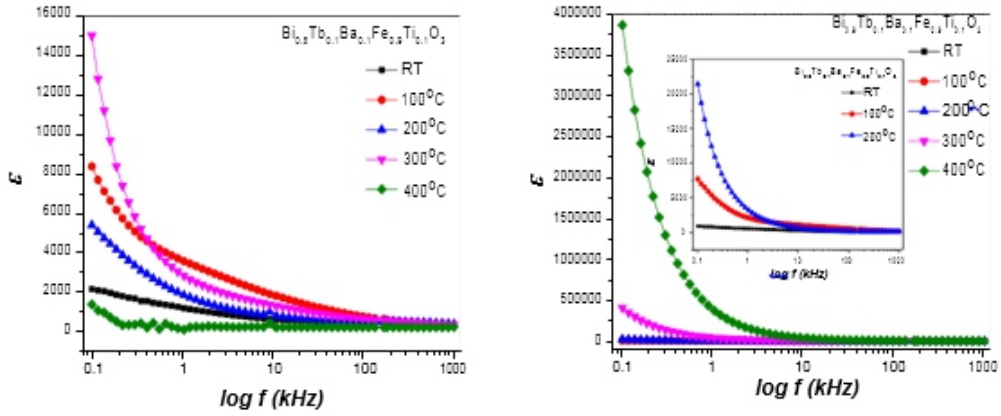

Fig. 4. Variation of real and imaginary part of (ε¢ and ε¢¢) dielectric constant as a function of frequency of Bi0.8Tb0.1Ba0.1Fe0.9Ti0.1O$_3$ceramic4s at different temperatures.

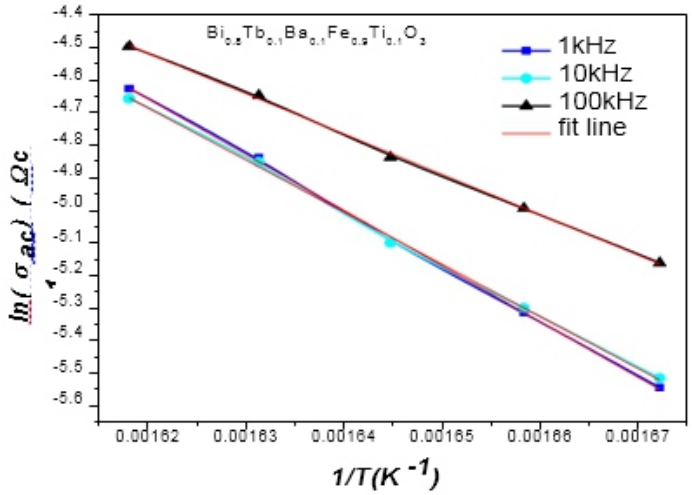

Fig. 5. Variation of ac conductivity (lnσac) as a function of absolute temperature (1/T) forBi0.8Tb 0.1 Ba0.1Fe0.9Ti0.1O3 ceramics at different frequencies (1kHz-100kHz).

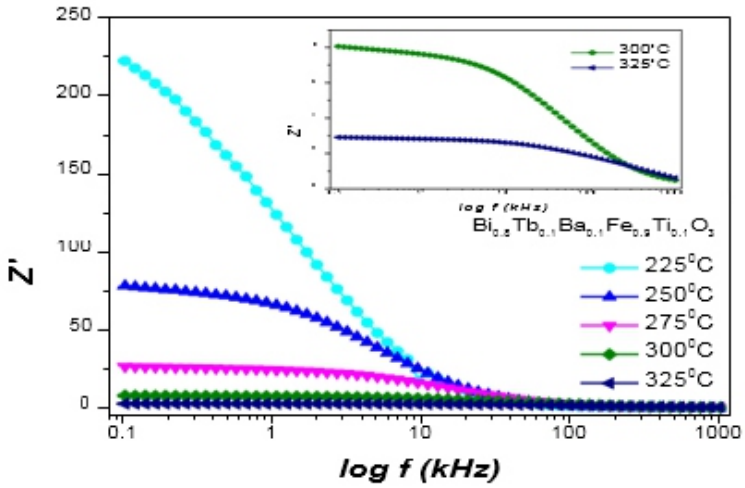

Fig. 6. Variation of real part of modulus (Z′) with frequency at different temperatures of Bi0.8Tb 0.1Ba0.1Fe0.9Ti0.1O3ceramics.

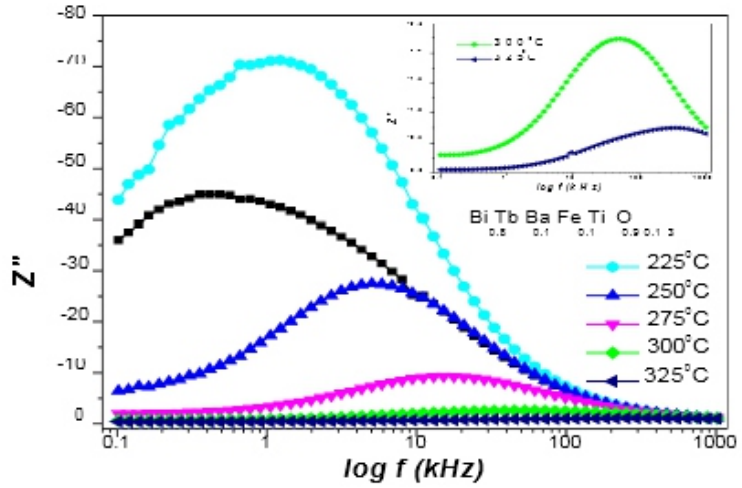

Fig. 7. Variation of imaginary part of modulus (Z′′) with frequency at different temperatures of Bi0.8Tb 0.1Ba0.1Fe0.9Ti0.1O3ceramics

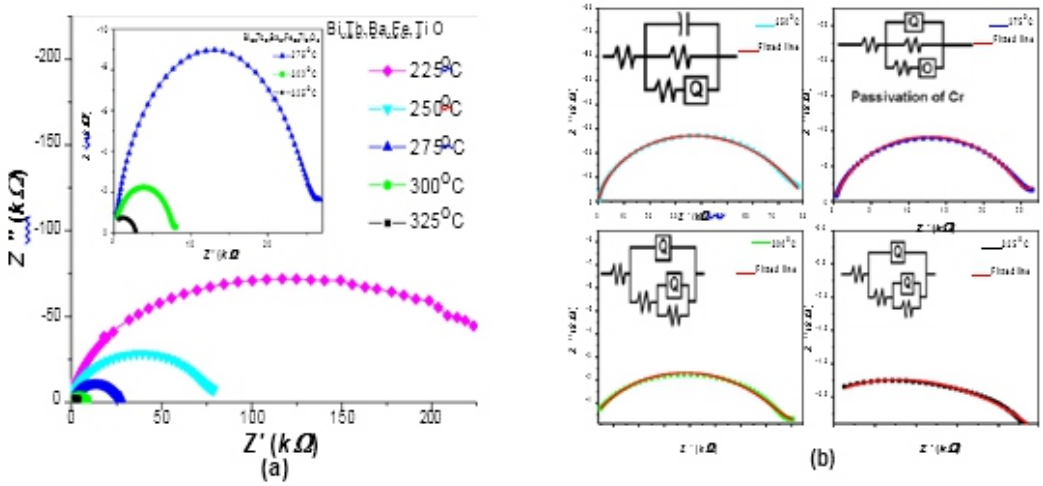

Fig. 8. (a)Variation of real and imaginary part (Z′ and Z′′) of impedance and (b) Fitted graph of real and imaginary part ((Z′ andZ′′) of impedance with different temperatures of Bi0.8Tb 0.1Ba0.1Fe0.9Ti0.1O3ceramics.

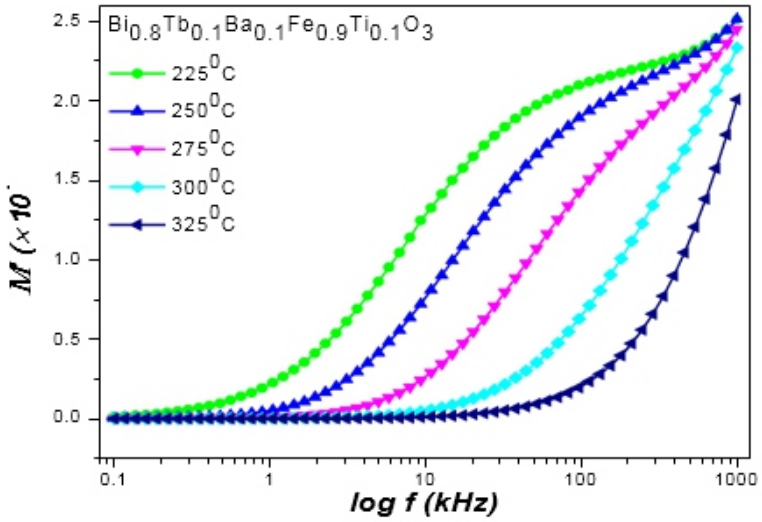

Fig. 9. Variation of real part modulus (M′) with frequency at different temperatures of Bi0.8Tb 0.1Ba0.1Fe0.9Ti0.1O$_3$ceramics.

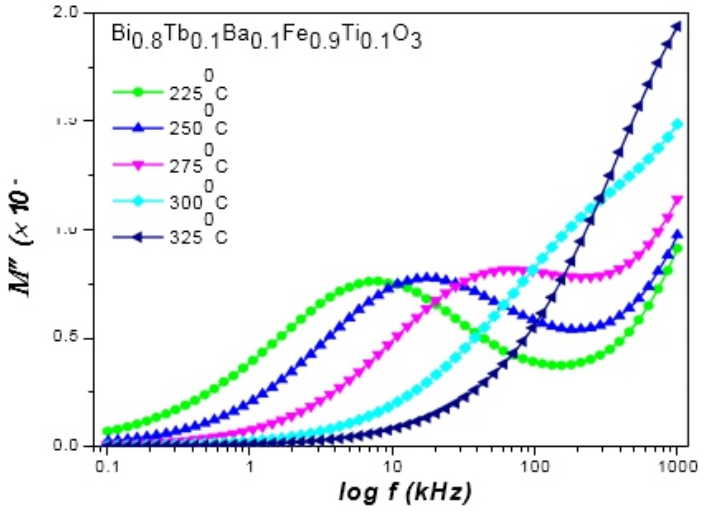

Fig. 10. Variation of imaginary part modulus (M′′) with frequency at different temperatures of Bi0.8Tb 0.1Ba0.1Fe0.9Ti0.1O3ceramics.

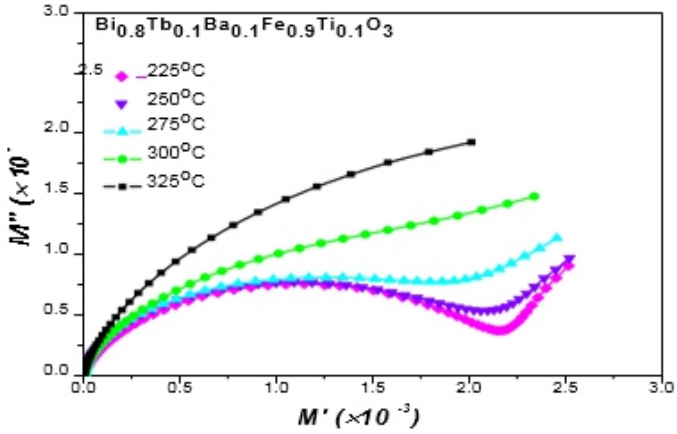

Fig. 11. Variation of real (M′) and imaginary part (M′′) of modulus with different temperatures of Bi0.8Tb 0.1Ba0.1Fe0.9Ti0.1O3ceramics.

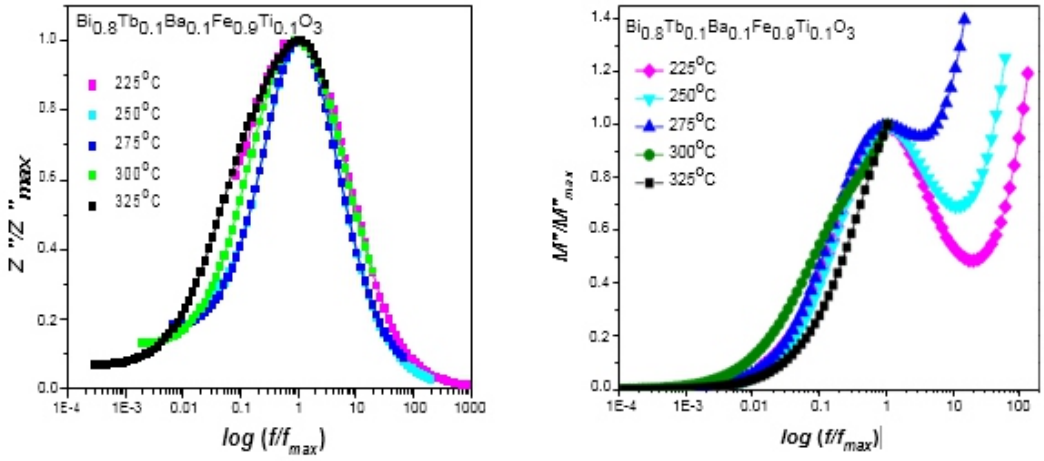

Fig. 12. Scaling behavior of (Z′′ / Z′′ max) and (M′′ / M′′ max) vs log (f/fmax) of Bi0.8Tb0.1Ba0.1Fe0.9Ti0.1O3ceramics.

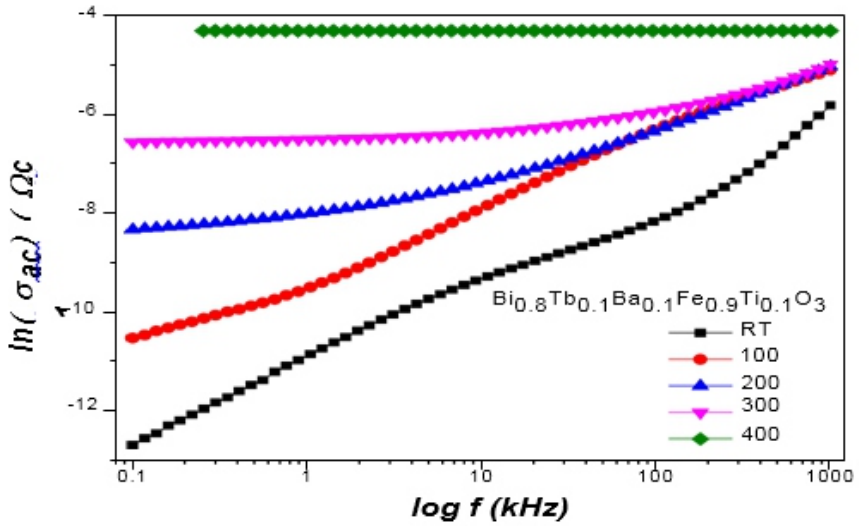

Fig. 13. Variation of lnσac (W/cm-1) vs. frequency of Bi0.8Tb0.1Ba0.1Fe0.9Ti0.1O3 ceramics at different temperatures.

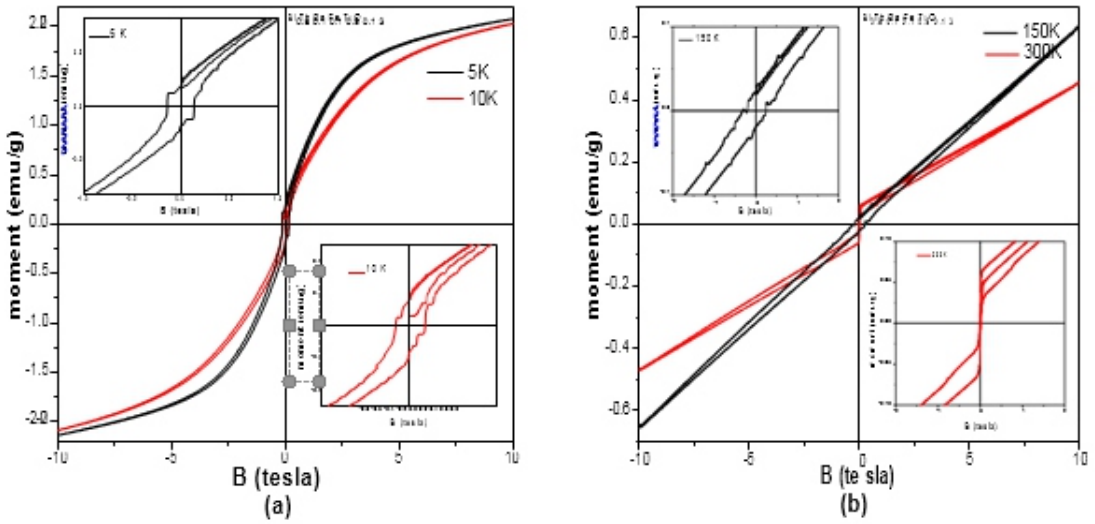

Fig.14. M–H loops of Bi0.8Tb 0.1Ba 0.1Fe0.9Ti0.1O3ceramics at (a)5K, 10K and(b)150K, 300K.

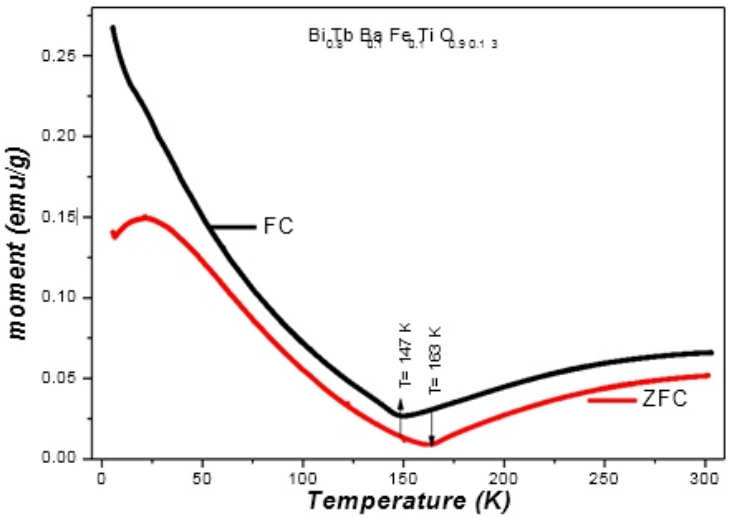

Fig.15.Variation of magnetic moment with temperature of Bi0.8Tb 0.1Ba0.1Fe0.9Ti0.1O3ceramics for FC and ZFC.

Periodical Effect of Cement Dust Pollution on Pea in the Vicinity of Banjari Cement Factory

Dr. Rajesh Kumar
Department of Botany,
V. K. S. University, Ara (Bihar)

ABSTRACT

The present work has been carried out under the impact of cement dust pollution in the vicinity of Banjari cement factory. The selected crop pisumsativum have been studies which grow under cement dust pollution Result of effect revealed to undergo stages of growth as compare to control crop.

Cement dust emittion from cement factory is essentially an inorganic mixture of oxide potassium, aluminium, silicon and sodium. These elements to change the physical and chemical properties of soil which is directly or indirectly they effect the normal growth of plant as well nutritive value of seeds.

Keyboard : Cement dust pollution cicer arietinum, NPK, cultivated Yield.

INTRODUCTION

The present investigation was carry out in the vicinity of Banjari Cement factory, Rohtas, Bihar where pea, i.e pisumsativumis being cultivated as rabi crop large quantities of cement dust, emitted in the area around the factory during crushing and pulserising of raw materials as well as during packing, loading and transporting of cement bag constitute a major threat to crop of this area. Cement dust emitting from a cement factory is essentially in inorganic mixture of oxides of calcium, potatssium, silicon and sodium these pollutants are found to adversely effect the standing crop biomass primary productivity, nutrient dynamics and enargetics. Strateman and Van Hant (1986) Shonbeck (1990) stated that dust falling on the soil caused shift in pH to the alkaline side so after the chemistry of soil.

Methods

For sampling of the cement dust, dust fail jars were used for settled dust and high volume sampler for suspended particles and similarly the foliar surface can be measured by collective dust fail in an area.

The first sampling of pisumsativum was done after 15 days and 30 days of the emergence of seeding. At each sampling date five plants were selected randomly and were dug out individually upto a depth of 30 cm. Plants were selected randomly and were dug out individually upto a depth of 30 cm. Plants were dried out in oven at 80^0 c for 48 hrs. The dried samples were weighed to estimate the biomass which were expressed in gm/cm2 similarly, the methods suggested by William (1970) and Misra (1962) were used to estimate the nitrogen and phosphorous contents in pea plants, Jackson (1962) methods was used to measure potassium sodium and calcium amount in plants.

RESULTS AND DISCUSSIONS

Plants samples were collected from control and polluted sites. The polluted site was elected in the north east direction of cement factory where dust load was zero. It was carried out during the period of 2011-12.

Seeds of pea were sown in rows in 4th week of October in the control and polluted sites. The samples were collected from both the sites at the age of 15, 30, 45, 60, 75 and 90 days internal from the date of sowing. The data collected were placed in the following table:

Table 1 : Mean Standing crop biomass (g/m^2) of pisumsativum on control site

Age (Days)	Aboveground (A)				Total	Under Ground (B)	Total (A+B)
	Stem	Leaf	Inf.	Standing Dead			
15	1.58	4.05	-	-	5.63	1.05	6.68
	±0.08	±0.38	-	-	±0.46	±0.08	±0.54
30	5.07	6.53	-	-	11.6	2.44	14.04
	±0.42	±0.61	-	-	±1.03	±0.21	±1.24
45	19.77	17.83	4.58	-	42.18	6.57	48.75
	±1.90	±0.02	±1.28	-	±3.20	±0.81	±4.01
60	108.64	43.65	7.68	-	159.97	13.22	173.19
	±12.01	±5.21	±2.38	-	±19.60	±1.26	±20.86
75	110.77	51.33	9.55	-	171.65	16.86	188.51
	±12.27	±5.69	±2.45	-	±20.41	±1.59	±22.00
90	114.19	50.93	10.48	5.29	180.89	20.78	201.67
	±12.66	±6.47	±1.18	±0.90	±21.21	±2.02	±23.23

Table 2 : Mean standing crop biomass (g/m2) of pisumsativum on polluted site

Age (Days)	Aboveground (A)				Total	Under Ground (B)	Total (A+B)
	Stem	Leaf	Inf.	Standing Dead			
15	1.27	3.34	-	-	4.61	0.84	5.45
	±0.06	±0.30	-	-	±0.36	±0.06	±0.42
30	4.08	5.26	-	-	9.34	1.96	11.3
	±0.33	±0.48	-	-	±0.81	±0.16	±0.97
45	15.92	14.34	3.12	-	33.38	5.28	38.66
	±1.52	±0.03	±0.82	-	±2.37	±0.65	±3.02
60	87.36	35.09	5.4	-	127.85	10.63	138.48
	±9.86	±4.18	±1.10	-	±14.92	±1.01	±15.93
75	89.06	41.28	8.2	-	138.54	13.56	152.1
	±9.86	±4.57	±2.20	-	±16.63	±1.28	±17.91
90	91.82	43.36	10.03	4.27	149.48	16.7	166.18
	±10.17	±5.20	±0.95	±0.80	±17.12	±1.63	±18.75

Fig. 5.1 : Stem Biomass of Pea at different age under control and polluted condition

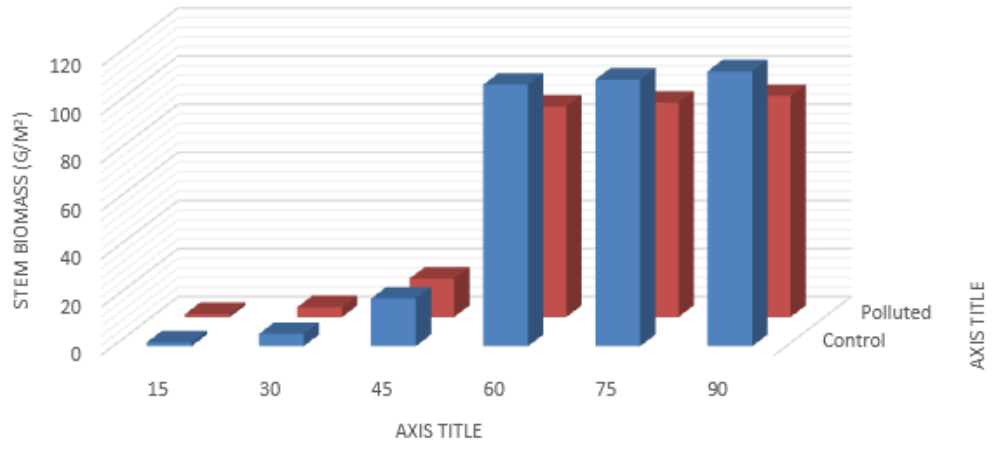

Fig. 5.1 : Leaf Biomass of Pea at different age under control and polluted condition

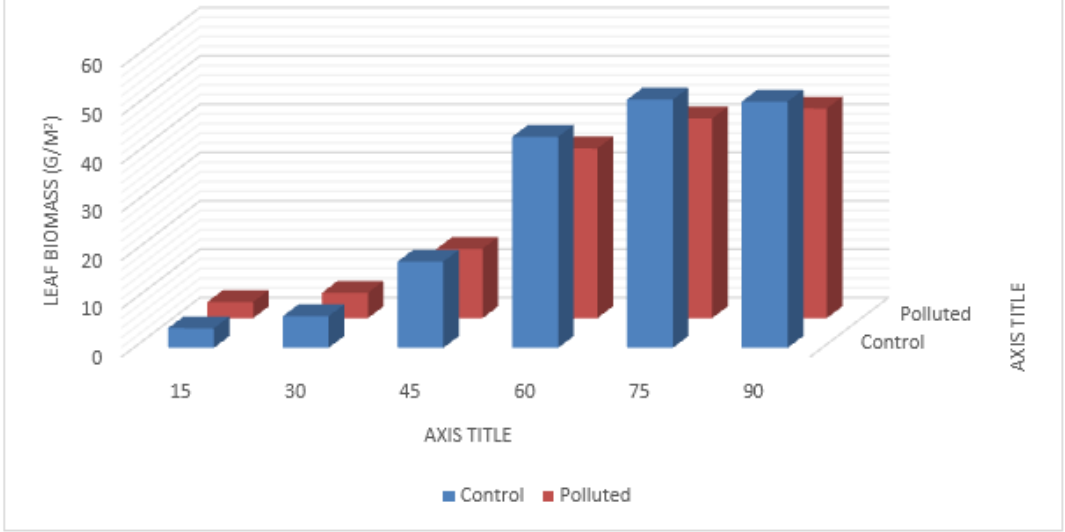

CONCLUSIONS

On the basis of this study it may be concluded that cement dust produces deleterious effects on growth and development of pulse yielding plants i.episumsativum. The cement dust affects the plants through encrustation of leaves, plugging of stomata, changes in quantum of light absorbed by leaves, change in pH both outside and inside of the leaf as well as through modification in soil condition. So, the above finding concludes the pea could suffer a loss in size and in terms of both quality and quantity in cement dust polluted area.

Conflicts of interest

Similarly the level of nitrogen, phosphorus, potassium, sodium and calcium in polluted plants at given age were less comparing to those in controlled plants. Perhaps the abundance of Ca++ions in cement dust affected soil decreases the nitrogen availability to plants (Demooy& Pesak1966). Excess calcium in soil may capture potassium and form calcium triphosphate and rendering it unavailable to plants (Devling 1975). Further, a possible incorporation of these cations through leaf surface could increase there levels in polluted plantns. (Bukovac&Wittwer S.H. 1957), (Levi, 1970), (Mc Farmland, J.C) and (Mc Farmland, 1971).

ACKNOWLEDGEMENTS

The cement dust after hydration and crystallization forms a hard on surface vegetation. It is already known that such a crust upset the growth and development of plants (Peirce 1909, Parish 1910, Czajal 1962). It was noted that the relative thickness of cement crust on pea plants from dusted to controlled sites was reduced. The crust occasionally got peeled off together with the cuticle exposing the dark green layer underneath. The incorporation of cement dust suspension containing Ca (OH)2 Al (OH)3 into the leaf tissue increase the pH of leaf tissue.

The biomass and primary productivity in polluted pea plants were constantly lower than those of controlled pea plants at all stages of growth and development. This reduction in the biological yield of polluted plants could be attributed to the cement dust which possibly affected the metabolism of pea in several ways.

REFERENCES

- *Bukovac, M.J. and Witter, S.H. (1957). Absorption and ability of foliage applied nutrients. Plant physiol.32: 428-435*
- *Jackson, M.L. (1962). Soil Chemical analysis, Prentice Hall Inc. Engle Wood Cliffs, N.J., USA*
- *Levi, E.(1970). Penetration, retention and transport of foliar applied single salts of Na,K, Pb, and Ca. Physiol. Plant. 23:811-819*
- *Mc Farblane, J.C. (1971). Curricular permeability to mineral nutrients. Ph.D. Dissertation, University of California, Riverside.*
- *Misra, R. (1968). Ecology Work Book. Oxford and BIG Publishing Company, New Delhi, 244.*
- *Bukovac, M.J. and Witter, S.H. (1957). Absorption and ability of foliage applied nutrients. Plant physiol.32: 428-435*
- *Williams, H. (1970). Officials methods of analysis of the association of occicial analytical chemist (ed.) Washington D.C.*
- *Decline, R.M (1975). Detection, occurrence and availability of the essential elements. In: Plant physiology. Affiliated East-West Press Pvt. Ltd., New Delhi.*

Instructions for Authors

Essentials for Publishing in this Journal

1 Submitted articles should not have been previously published or be currently under consideration for publication elsewhere.

2 Conference papers may only be submitted if the paper has been completely re-written (taken to mean more than 50%) and the author has cleared any necessary permission with the copyright owner if it has been previously copyrighted.

3 All our articles are refereed through a double-blind process.

4 All authors must declare they have read and agreed to the content of the submitted article and must sign a declaration correspond to the originality of the article.

Submission Process

All articles for this journal must be submitted using our online submissions system. http://enrichedpub.com/ . Please use the Submit Your Article link in the Author Service area.

Manuscript Guidelines

The instructions to authors about the article preparation for publication in the Manuscripts are submitted online, through the e-Ur (Electronic editing) system, developed by **Enriched Publications Pvt. Ltd**. The article should contain the abstract with keywords, introduction, body, conclusion, references and the summary in English language (without heading and subheading enumeration). The article length should not exceed 16 pages of A4 paper format.

Title

The title should be informative. It is in both Journal's and author's best interest to use terms suitable. For indexing and word search. If there are no such terms in the title, the author is strongly advised to add a subtitle. The title should be given in English as well. The titles precede the abstract and the summary in an appropriate language.

Letterhead Title

The letterhead title is given at a top of each page for easier identification of article copies in an Electronic form in particular. It contains the author's surname and first name initial .article title, journal title and collation (year, volume, and issue, first and last page). The journal and article titles can be given in a shortened form.

Author's Name

Full name(s) of author(s) should be used. It is advisable to give the middle initial. Names are given in their original form.

Contact Details

The postal address or the e-mail address of the author (usually of the first one if there are more Authors) is given in the footnote at the bottom of the first page.

Type of Articles

Classification of articles is a duty of the editorial staff and is of special importance. Referees and the members of the editorial staff, or section editors, can propose a category, but the editor-in-chief has the sole responsibility for their classification. Journal articles are classified as follows:

Scientific articles:

1. Original scientific paper (giving the previously unpublished results of the author's own research based on management methods).

2. Survey paper (giving an original, detailed and critical view of a research problem or an area to which the author has made a contribution visible through his self-citation);

3. Short or preliminary communication (original management paper of full format but of a smaller extent or of a preliminary character);

4. Scientific critique or forum (discussion on a particular scientific topic, based exclusively on management argumentation) and commentaries. Exceptionally, in particular areas, a scientific paper in the Journal can be in a form of a monograph or a critical edition of scientific data (historical, archival, lexicographic, bibliographic, data survey, etc.) which were unknown or hardly accessible for scientific research.

Professional articles:

1. Professional paper (contribution offering experience useful for improvement of professional practice but not necessarily based on scientific methods);
2. Informative contribution (editorial, commentary, etc.);
3. Review (of a book, software, case study, scientific event, etc.)

Language

The article should be in English. The grammar and style of the article should be of good quality. The systematized text should be without abbreviations (except standard ones). All measurements must be in SI units. The sequence of formulae is denoted in Arabic numerals in parentheses on the right-hand side.

Abstract and Summary

An abstract is a concise informative presentation of the article content for fast and accurate Evaluation of its relevance. It is both in the Editorial Office's and the author's best interest for an abstract to contain terms often used for indexing and article search. The abstract describes the purpose of the study and the methods, outlines the findings and state the conclusions. A 100- to 250-Word abstract should be placed between the title and the keywords with the body text to follow. Besides an abstract are advised to have a summary in English, at the end of the article, after the Reference list. The summary should be structured and long up to 1/10 of the article length (it is more extensive than the abstract).

Keywords

Keywords are terms or phrases showing adequately the article content for indexing and search purposes. They should be allocated heaving in mind widely accepted international sources (index, dictionary or thesaurus), such as the Web of Science keyword list for science in general. The higher their usage frequency is the better. Up to 10 keywords immediately follow the abstract and the summary, in respective languages.

Acknowledgements

The name and the number of the project or programmed within which the article was realized is given in a separate note at the bottom of the first page together with the name of the institution which financially supported the project or programmed.

Tables and Illustrations

All the captions should be in the original language as well as in English, together with the texts in illustrations if possible. Tables are typed in the same style as the text and are denoted by numerals at the top. Photographs and drawings, placed appropriately in the text, should be clear, precise and suitable for reproduction. Drawings should be created in Word or Corel.

Citation in the Text

Citation in the text must be uniform. When citing references in the text, use the reference number set in square brackets from the Reference list at the end of the article.

Footnotes

Footnotes are given at the bottom of the page with the text they refer to. They can contain less relevant details, additional explanations or used sources (e.g. scientific material, manuals). They cannot replace the cited literature.
The article should be accompanied with a cover letter with the information about the author(s): surname, middle initial, first name, and citizen personal number, rank, title, e-mail address, and affiliation address, home address including municipality, phone number in the office and at home (or a mobile phone number). The cover letter should state the type of the article and tell which illustrations are original and which are not.

Address of the Editorial Office:

Enriched Publications Pvt. Ltd.
S-9,IInd FLOOR, MLU POCKET,
MANISH ABHINAV PLAZA-II, ABOVE FEDERAL BANK,
PLOT NO-5, SECTOR -5, DWARKA, NEW DELHI, INDIA-110075,
PHONE: - + (91)-(11)-45525005

Note